8-2013

Experimental Development and Analysis of a Novel Setup for Insulated Dielectrophoresis

Johnie Hodge
Clemson University, johnieh@g.clemson.edu

EXPERIMENTAL DEVELOPMENT AND ANALYSIS OF A NOVEL SETUP FOR INSULATED DIELECTROPHORESIS

A Thesis
Presented to
the Graduate School of
Clemson University

In Partial Fulfillment of the
Requirements for the Degree
Master of Science
Bioengineering

---

by:
Johnie O'Neil Hodge
August 2013

Accepted by:
Dr. Guigen Zhang, Committee Chair
Dr. Bruce Gao
Dr. Xiangchun Xuan

ABSTRACT

Dielectrophoresis has long been studied and utilized for the manipulation of microscale particles in solution. This phenomenon is due to the induced polarization of dielectric particles subjected to an electric field. When the field is also inhomogeneous in terms of the distribution of its strength through space, the polarized particles move and come to rest in certain areas due to the relationship between their and the solvent's relative permittivities. If the electric field is homogenous, such as within a parallel plate capacitor, the particles are polarized according to their permittivity and the field's frequency, but they will not move.

These relationships have been exploited for many lab-on-a-chip applications such as positioning cells for tissue engineered structures, separating live cells from dead ones, or separating cells of different types. Some of these systems also employ microfluidics in order to add another level of control, increasing the degrees of freedom when manipulating microparticles.

The goals of this study are to develop and experimentally characterize a low power setup for moving and aligning particles using dielectrophoresis, to perform experiments to quantify the effect of conductivity on the dielectrophoretic force, to analyze and quantify the out of plane force, and to use these experimentally determined relationships to create more accurate theoretical models of dielectrophoresis processes using COMSOL Multiphysics software.

The first step in this process involves the creation of a technique to perform dielectrophoresis using relatively low power. This requires the use of a very thin, durable

membrane to separate the particles in solution from the field generating electrodes. The use of this very thin membrane, much thinner than those used in previous studies,[1] has revealed a much more complete picture of the behavior of microparticles in response to the forces present during dielectrophoresis. A more complete picture of reality has the potential to lead to the creation of more accurate models and descriptions of the underlying physics.

Once this novel setup was shown to produce consistent results, the studies began. These consisted largely of frequency sweeps at constant voltages and voltage sweeps at given frequencies, similar in basic method to studies which have been performed to analyze dielectrophoretic systems in the past.[2, 3] No flow is present in the particle suspension for the majority of these studies. This constraint, coupled with the insulating layer over the electrode theoretically limits the forces present to principally those elicited by dielectrophoresis.

With this setup it was found that polystyrene beads were arranged into parallel lines of pearl chains in the spaces between interdigitated electrodes with sufficient predictability that models of this phenomenon could be created and aligned with reality. In addition to these in-plane forces governing the formation of pearl chains, the out of plane forces were also analyzed and modeled. In the case of negative dielectrophoresis, this is the force lifting the beads off of the electrode surface. The effect of media conductivity on particle alignment and levitation has also been analyzed using this setup. In addition to these experiments with polystyrene beads, this setup has also been shown to manipulate cells under low media conductivity conditions.

It is important that the forces and physical relationships involved in these insulated dielectrophoresis setups are better understood, so that such techniques can be more precisely and predictably implemented for lab-on-a-chip and tissue engineering applications.

ACKNOWLEDGEMENTS

I most sincerely appreciate the insight and continued support of my advisor and committee chair Dr. Guigen Zhang. To my other committee members, Dr. Xiangchun Xuan and Dr. Bruce Z. Gao, I offer my thanks for your advice and in the case of Dr. Gao, the regular use of the clean room.

I offer a special thanks to Nrutya Madduri and especially Dr. Rajan Gangadharan, who mentored me when I first began my undergraduate research and taught me so much about the research process. Yu Zhao and Vandana Devi have put a great deal of work into topics similar to my own research focus; it has been a wonderful experience working with you both so closely. I would also like to thank Dr. Michael Bridgwood and Dr. Daniel Noneaker for their advice and referrals on all matters electrical, and Dr. Vladimir Reukov, Dr. Guzeliya Korneva, and Aby Thyparambil for their help in analyzing the parameters of my experimental setup. The financial support from Tokyo Electron US Holdings is greatly appreciated.

TABLE OF CONTENTS

LIST OF FIGURES

Page

CHAPTER ONE

INTRODUCTION

1.1 Background

Dielectrophoresis is defined as the polarization and corresponding motion of dielectric particles due to their interaction with an inhomogeneous electric field. This interaction takes two principal forms, visually characterized by motion toward or away from the electrode edges. Motion toward the electrode edges in a planar electrode setup (up the electric field gradient) is called positive dielectrophoresis, while motion away from the electrode edges (down the field gradient) is termed negative dielectrophoresis. The physical explanation for these two categories of polarization is a rather simple one, and is illustrated in **Figure 1.1** below. It is important to note that this figure only depicts polarization, as the field distribution is homogeneous.

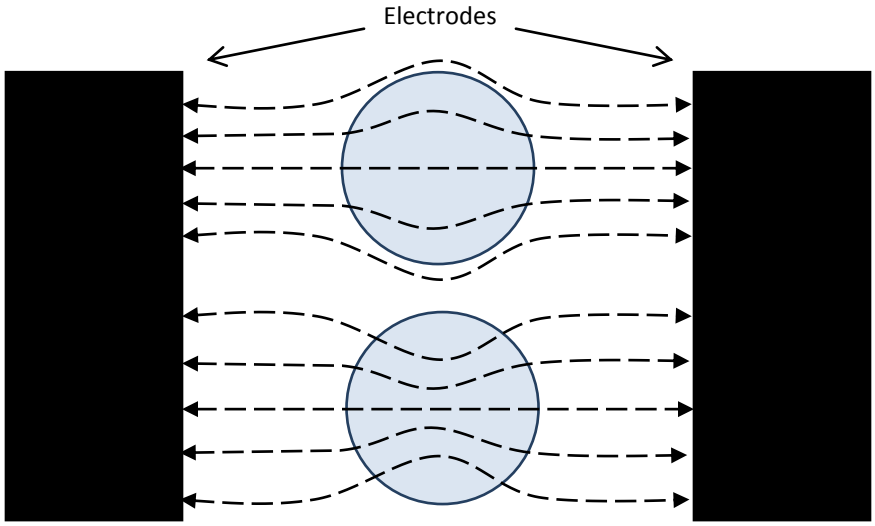

Figure 1.1: Illustration of polarization; Particle A above; Particle B below

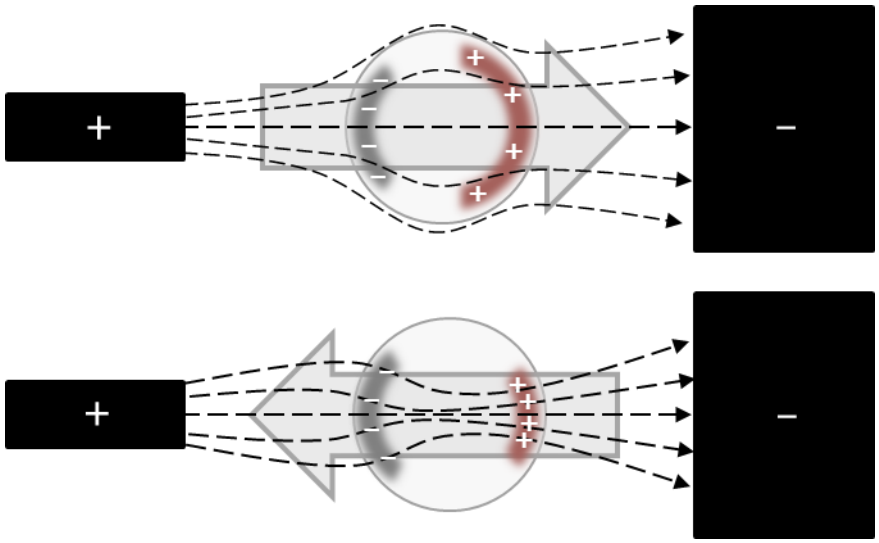

Figure 1.2: Illustration of dielectrophoresis;
Particle A [-] above; Particle B [+] below

When a particle is placed in a nonuniform electric field it responds as follows. If the relative permittivity of the particle is lower than that of the media in which it is suspended, then the field will be distorted around the particle in such a way as to produce an area of lower electric field line density in the space that the particle occupies (**Figure 1.1: Particle A**). When the field is nonuniform, the system will move toward equilibrium, thus the particle containing lower field line density will move in the direction of decreasing density in the surrounding field (**Figure 1.2: Particle A**). In contrast, if a particle has a higher polarizability in comparison with the solvent in which it is suspended, it will move in the direction of increasing field line density due to the same phenomenon. The field lines will be distorted by the particle in such a way that they will be concentrated in the particle (**Figure 1.1: Particle B**). As the system moves toward equilibrium, the particle is pulled up the field gradient, toward regions of increasing field

strength (**Figure 1.2: Particle B**). However, such motion is only possible when the dielectric particles are exposed to a time varying field. This is because the frequency of the field must be properly tuned to induce the initial polarization of dielectric particles. If the field is homogenous, but varying, theory dictates that the particle will still be polarized, though it will not move due to the lack of a significant field gradient **Figure 1.1**.

The schematic depicted in **Figure 1.2** was verified using COMSOL. The following figure is an arrow plot showing the electric field line distortion induced by the beads.

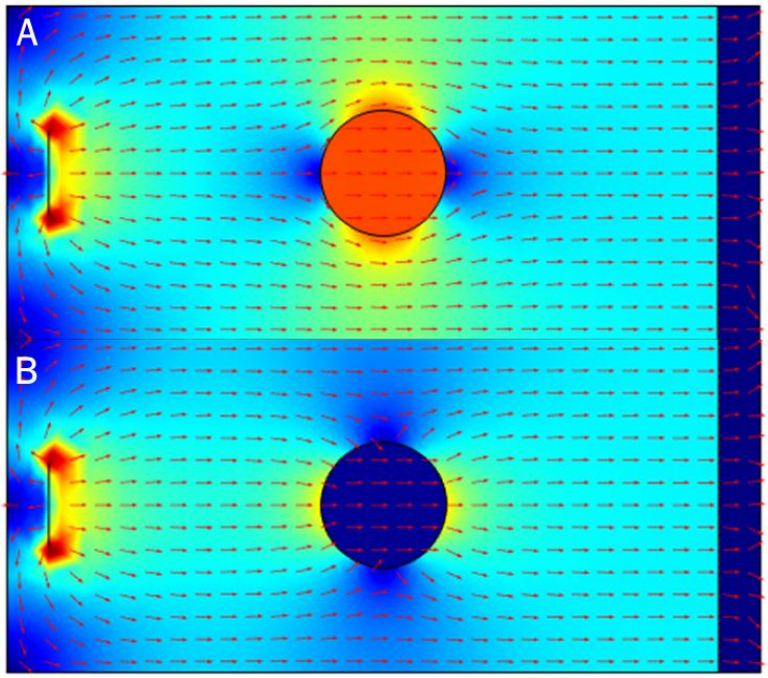

Figure 1.3: COMSOL model of DEP field distortion;
Particle A [-] above; Particle B [+] below

1.2 Objectives and Motivation

The primary objectives of these studies are to design a setup for performing low power dielectrophoresis, to investigate the properties of such a setup in terms of the frequency responses of differ sized polystyrene beads, to quantify the dielectrophoretic force in the vertical direction perpendicular to the electrode surface, and to experimentally quantify the effect of media conductivity on the magnitude of the effective dielectrophoretic force. Computer models will then be constructed of similar situations in order to more thoroughly test the practical veracity of theoretical equations and descriptions of physical factors.

In the majority of dielectrophoresis setups, there is direct contact between the electrodes and the aqueous media in which the particles are suspended. This is theoretically a perfectly viable option as long as media composition and voltage levels are tightly controlled. If the conductivity of the media rises due to ions released from cells or some other source, the resulting ionic currents could lead to electrolysis of the aqueous media and subsequent oxidative damage to the electrode surface. In addition to this drawback, if biological material is being manipulated, the electrode itself will become contaminated when used and must be disposed of or cleaned. Cleaning these delicate electrodes often results in irreparable damage, and it would be considerably cheaper to reuse the electrodes instead of using a new one for each operation.

The primary setup discussed here solves this problem by making use of a thin (~12.7μm thick) sheet of low density polyethylene (LDPE) to cover the electrode. The membrane along with low media conductivity, decrease the activity of other forces such

as electrophoresis, electro-osmosis, and convection due to joule heating. This sheet can be removed and disposed of so that the electrode can be reused immediately. It is also likely that this material could be treated in some fashion to be used as a substrate for simply culturing the cells or allow them to be easily transferred to another system intended to monitor or manipulate them for some further purpose. The main design goals are reusability, preservation of the electrode, and repeatable low-voltage insulated dielectrophoretic manipulation of microparticles. This setup design will be rigorously analyzed through the characterization of the frequency response of polystyrene beads.

Once the design proves reliable, a particular area of study will be the dielectrophoretic force in the z-direction (if the surface of the electrode is considered the XY-plane). This force has not been extensively analyzed during negative dielectrophoresis, and such an analysis would contribute to a deeper understanding of the underlying physics. The effect of media conductivity on this “levitation force” will also be quantified. The final goal is to demonstrate that this setup is capable of aligning cells. This is a widely performed and particularly important application of dielectrophoresis.

CHAPTER TWO

LITERATURE REVIEW

2.1 An Overview of Dielectrophoresis Experimentation

The scientific principles governing dielectrophoresis have been largely understood since 1873 due to the work of John Clerk Maxwell.[4] However, the first serious study of this specific phenomenon did not begin until the 1950's.[5] Herbert A. Pohl was the first to truly study dielectrophoresis, and provided the principal governing force equation still accepted today. This equation is discussed further in **Chapter 3** where it appears as **Equation 9**. The majority of these past studies of dielectrophoresis either attempt to explain elements of the underlying physics or apply the technique of dielectrophoresis to accomplish a particular goal such as cell manipulation or the determination of a particle's electrical properties. The application studies seldom contain substantial theoretical examinations of their setups. As the physics behind dielectrophoresis has become better understood, there has been a movement toward producing many more application studies with only cursory mentions of theory.

A fairly comprehensive overview of the development of this field up to the present is compiled by Ronald Pethig.[6] He writes what is largely a review article and takes many of the published works available at the time (1996) and summarizes most of the relevant factors influencing the dielectrophoretic behavior of particles in solution that have been elucidated by these works. The chief aim of the majority of the studies which are analyzed is the dielectrophoretic separation of various cells and microorganisms. At the time this work was compiled, scientists had just begun to use microfabricated

electrodes patterned via photolithography for biomedical, biochemical and biotechnological applications such as monitoring and manipulating cells.

The basic explanations of dielectrophoretic theory contained in this paper are concise and provide more of a spatial understanding of the physics involved rather than a simply mathematical one, though the force equation (similar to **Equation 9**) is provided and explained in the context of the range of possible theoretical relationships between the media and particles' relative polarizabilities.

An informative history of the progression of the field of dielectrophoretic manipulation of bioparticles is presented beginning with the pioneering studies of Pohl. The work of Irwin P. Ting et al. with chloroplasts represents a relevant example of the very early studies performed in the dielectrophoresis of bioparticles;[7] Herbert A. Pohl is one of the authors, though these experiments are a good deal more narrowly focused and refined than his pioneering work. Here, the study is aimed at seeing whether particles as small and delicate as chloroplasts can be collected from solution using positive dielectrophoresis.

In Ting's study,[7] Dielectrophoresis is performed by applying 50Vpp (peak-to-peak amplitude of the voltage), which is significantly greater than similar studies of larger particles, across a setup consisting of two rounded platinum electrode tips 425μm in diameter projecting into the chloroplast suspension and separated by a distance of 850μm. This system resulted in two strong peaks of chloroplast aggregation at the electrode-fluid interface at 300Hz and 1MHz. While the 1MHz peak is perfectly acceptable according to dielectrophoresis theory, the 300Hz peak is very unusual and is

hypothesized to be because of the extremely large surface area of the grana available for Helmholtz double-layer formation, but this is a hypothesis that is not directly tested in this particular paper. There is also a smaller aggregation peak at 3×10^{7}Hz further pointing to the complexity of the system. Interestingly, when the setup was kept in the dark, or stabilized with DCMU, the aggregation response was more pronounced. Both of these treatments theoretically prevent photosynthetic activity.

This observation, coupled with the further recognition that the aggregation of chloroplasts disperses after about 30 minutes, points to the release of charged substances from the chloroplasts, raising the conductivity over time and therefore increasing the polarizability of the media and increasing the strength of several competing forces (such as AC electro-osmosis) and consequentially decreasing the overall effectiveness of the positive dielectrophoretic attraction force. This reasoning is not provided in this early paper, but such explanations are given for this phenomenon in more recent works.[8]

The results of Kaler and Jones from the early 1990s in which they used positive dielectrophoresis and an electronic feedback system to maintain the levitation of cells in aqueous media are discussed by Pethig.[9,10,11] Systems utilizing negative dielectrophoresis for particle manipulation and alignment were subsequently devised and implemented, often in conjunction with microfluidics due to the fact that when the particles are held away from the electrode, they are more easily removed by fluid flow.

Some studies where very small particles are aligned such as those of Washizu and Fuhr have shown that it is possible to manipulate proteins, DNA, and single viruses by using very large electric fields.[12, 13, 14] Fuhr also presents a system for levitating cells

using positive dielectrophoresis,[3] and Washizu and Jones present an expansion of traditional dielectrophoretic theory to account for such behavior.[15] The final group of studies outlined by Pethig which could be pertinent to our goals are those of Becker, Markx, and Stephens demonstrating that several cell types (erythrocytes, yeast, and CD34+ cells respectively) remain viable after exposure to the electric fields required for dielectrophoretic manipulation.[16, 17, 18, 19] Our setup would seem to provide even more protection for the cells, but if it is to be applied as part of a system for cell manipulation, similar studies to these would likely need to be performed.

Before the advent of relatively advanced and easy to use finite element analysis software such as COMSOL, there was still a desire to gain an understanding of the strength and distribution of the local electric field around dielectrophoretically aligned cells. Mehrle et al. use bacteria and chloroplasts, as well as very small glass and polystyrene beads as field probes in attempts to loosely map the field line distribution around much larger plant protoplasts.[20]

The first key piece of insight that Mehrle's work provides is that the simultaneous introduction of large and small particles reduces the field strength necessary for the manipulation of particles the size of chloroplasts or bacteria. According to the previously discussed paper by Ting et al., the power of the signal necessary for reliable manipulation of chloroplasts was six times higher than that required for attracting a moderately sized eukaryotic cell.[7] At the same time, it is assumed that the small sizes of the various particles in comparison to that of the protoplasts will ensure that their introduction into

the system will not cause field distortion significant enough to affect the global distribution of the fields surrounding the protoplasts.

The setup for Mehrle's studies involves the use of two NiCr wires attached to a glass slide about 200µm apart in parallel functioning as the only electrodes. The media containing the protoplasts consists of a 1:1 ratio of sorbitol/sucrose with the low conductivity of 10µS/cm.

Above a field strength of about 70V/cm at 1MHz frequency, the protoplasts are aligned due to positive dielectrophoresis. The inactivated *Pseudomonas aeruginosa* bacteria are introduced into the system and form extensions from the poles of single protoplasts in the directions of the electrodes and aggregate between protoplasts which have formed chains across the gap between the electrodes. This alignment of bacteria highlights regions of higher field strength due to the distortions induced by the presence of the protoplasts.

The introduction of polystyrene beads into the solution resulted in the formation of equatorial rings around the protoplasts. These beads, having a lower polarizability than the surrounding media and the cells, aggregate at regions where the field strength is the lowest. Thus, there must be a region of induced low field strength around the equator of each of the protoplasts.

In addition to understanding the effects of dielectric particles on electric field distribution, it is important to understand the effect that other physical parameters have on the efficacy of dielectrophoresis. Fomchenkov et al. present a report of their studies involving optical registration measurements of dielectrophoretic systems.[21] They also

demonstrate the frequency dependence of dielectrophoresis is itself conductivity and pH dependent.

Their studies are carried out in a sealed fluidics chamber containing wire electrodes and low conductivity media consisting of sucrose, sorbitol, and albumin in DI water. Erythrocytes and *Pseudomonas fluorescens* are used in the experiments which support what was then a relatively new theoretical description of dielectrophoretic force advanced by Pohl.

In addition to the results reported, there is a great deal of information to be gleaned from the introduction. This begins with a discussion of low tech measurement techniques, one of which involves attracting a cell onto an electrode via positive dielectrophoresis and lowering the voltage until it releases and falls away due to gravity. This method is somewhat reversed in our voltage sweep studies intended to quantify the out-of-plane dielectrophoresis force outlined in **Chapter 4**. The force that our study seeks to quantify is due to negative dielectrophoresis.

In setups designed for performing dielectrophoresis, it is often the case that other electrokinetic forces are at work. This is especially true if the media conductivity is to be raised, and the effects of such action studied.[2]

The work of Seungkyung Park et al. provides a tested and in-depth quantitative description of the roles of various physical processes potentially involved in dielectrophoresis setups.[8] The system proposed here is intended to provide a framework for designing predictably functioning electrokinetic setups for manipulating microparticles.

The study itself begins with the experimental section. The setup for these studies involves simple interdigitated electrodes with 30μm spacing fabricated using conventional photolithographic techniques. The fluid chamber is constructed using a 1mm thick O-ring covered by a glass coverslip. Three types of particles (gold, polystyrene, and *Clostridium sporogenes* bacteria) are used in these studies in order to obtain a relatively complete description of possible outcomes to be observed. All studies are performed at 10Vpp in the frequency range of 0~100MHz.

The results of these studies are compared with a scaling analysis, which takes into account four principal forces: dielectrophoresis, electrophoresis, AC electro-osmosis, and Brownian motion. This analysis results in the prediction of the dominant forces in interdigitated systems with various combinations of conductivity and frequency using each of the three types of particles. These predictions of dominant force are displayed in phase diagrams with frequency on the ordinate and media conductivity on the abscissa. Such predictions and methods are invaluable in the design and implementation of dielectrophoretic manipulation systems.

Park et al. also demonstrate that electrodes can be designed in such a way to take advantage of electrothermal flow patterns to enhance the efficacy of negative dielectrophoresis based trapping of latex and silica particles.[21] The reason for attempting dielectrophoresis in high conductivity media is that for cells to be kept alive for any significant period of time there must be a relatively large quantity of ions in their surrounding media.

The studies are performed on their modified interdigitated electrode, which essentially functions to trap piles of beads in open areas within the digits of each electrode. The media conductivities tested are 10^{-5}S/m (DI water), 0.05S/m (3.8mM NaCl), and 0.224S/m (17mM NaCl). An oscillating potential of 10Vpp at a frequency of 10MHz is applied to the media at each conductivity level. The results of these studies show that it is indeed possible to trap particles with low relative permittivity in such an electrode array at conductivities up to 0.224S/m. The aggregation of both latex beads and silica particles decreased in intensity with increasing conductivity, but substantial aggregation still occurred in agreement with the predictions they made from numerical simulations as well as the scaling method outlined in the work discussed immediately previous to this one. This method did predict whether or not aggregation would occur, but did not characterize the intensity of the aggregation to be expected.

It is important to note that there are very few studies performed in high conductivity media due to the fact that dielectrophoresis is less effective and there is significant risk of damaging the electrodes when they are in direct contact with the solution.

Though the two previously discussed studies are largely intended to advance a theoretical interpretation of dielectrophoretic chip design, they do present significant experimental support for their claims. In addition to studies dealing with the theory of dielectrophoresis and other electrokinetic forces, there has also recently been an increased desire to apply the technique of dielectrophoresis to areas such as tissue engineering. The following study performed by Chen-Ta Ho et al. focuses on a direct tissue engineering

application for dielectrophoretic manipulation of cells.[22] Here a process is outlined for controlling the alignment of hepatocytes due to positive dielectrophoresis in low conductivity media consisting of only 8.5% sucrose and 0.3% glucose. The circular interdigitated electrodes are patterned so that they have tooth-like projections where it is desired that a chain of cells should form a bridge between adjacent digits. The purpose of aligning the hepatocytes in this way is to mimic the structural arrangement of a lobule, the basic functional unit of liver tissue.

The patterned electrode is housed in a rather complex microfluidics chamber. This allows for the low conductivity media, required for effective positive dielectrophoresis, in which the cells are initially suspended to be replaced with high conductivity growth media, leaving the cells relatively undisturbed.

Using 5Vpp at a frequency of 1MHz, with the cell suspension in direct contact with the electrode, predictable alignment in the designed radial pattern was achieved. Additional results show that a mixture of hepatocytes and endothelial cells could be heterogeneously aligned, further adding to the complexity of the engineered tissue. Cells are also shown to be viable after arrangement and adhesion.

In bringing the discussion of dielectrophoretic experimentation closer to the studies presented in this document as a whole, Kidong Park et al. propose the use of a setup that is in many ways similar to the one we have developed and analyzed.[1] The purpose of their work is to bring down the cost of dielectrophoresis by patterning their interdigitated electrodes on printed circuit boards (PCBs) and making use of a 100μm thick glass coverslip to separate the electrode from the particle suspension (though there

is a thin film of DI water between the coverslip and the electrode), thereby allowing the electrode to be reused.

Their studies are conducted at 76Vpp with a frequency of 1MHz using both polystyrene beads and HeLa cells. The results presented show that various forms of alignment are possible, but do little more than this and in doing so invite deeper investigation of the operation and potential applications of similar techniques. It is also the case that when such high voltages are used there is significant electrolysis in the water layer used to improve contact between the glass coverslip and the electrode.[22] This could damage the electrode removing the prospect of its reuse. The presence of electrolysis also indicates the passage of current between electrode terminals. Even a small amount of current at such high potentials could produce an undesirable dissipation of power into the system.

2.2 Research Focus

In the context of the studies presented in the previous section, it is more apparent how our study fits into the field as a whole. There has been little in-depth work done to investigate the operation of insulated dielectrophoresis setups. The force levitating low permittivity particles off of a planar electrode due to negative dielectrophoresis has not been quantified, and nor has the effect of conductivity on this levitating force been systematically studied. We investigate some of these issues and principles further and some relatively practical solutions are presented by combining and altering the techniques discussed in the papers reviewed here.

For example our conductivity analysis is somewhat similar to that described above.[2, 21] Ours differs in that significantly more media conductivities are tested, and our results are in terms of levitation voltage. This is much more straight-forwardly quantifiable than particle aggregation density. In addition to this, the levitation studies found in literature all deal with positive dielectrophoresis, and while they are analyzing a similar principle there are significant differences in both experimental method and setup.

Our setup design is novel, though it bears significant similarity to that used by Park et al.[1] One crucial way in which our design is an improvement on their setup is that uses far less power. They were using voltages as high as 76Vpp and enough current passed through the DI water under the glass coverslip insulating the electrode from the solution that significant electrolysis was observed. Our much thinner LDPE sheet allows for much smaller voltages to be used (~6Vpp) and therefore virtually eliminates the danger of electrolysis. The SU-8 coated setup passes no current of any kind between the electrode digits and thus effectively dissipates no power.

Even though the frequency sweeps performed are similar to those that have been performed for many years on various setups,[2] they are very important in the characterization of our novel setup.

Additionally, our levitation voltage measurements use a novel technique, and to our knowledge, no one has quantified the force in the z-direction for negative dielectrophoresis. The technique that we use in somewhat similar in its simplicity to that discussed by Fomchenkov for measuring the strength of a positive dielectrophoretic force, but it is quite different in it application.[2]

CHAPTER THREE

THEORETICAL EXPLANATIONS OF CONCEPTS

3.1 Dielectrophoresis in Detail

Dielectrophoresis is a key component of the electromechanics of small particles in solution. In order for this process to occur, the particle must first be polarized through interaction with an electric field $\boldsymbol{E_o(r)}$, a function of distance from the source charge. The particles are taken to be suspended in a homogeneous dielectric fluid. Both this particle and the fluid media have complex permittivities, which are functions of frequency and can each be represented with the form $\varepsilon^*(\omega) = \varepsilon'(\omega) + i\varepsilon''(\omega)$, where $\varepsilon''(\omega) = \frac{\sigma}{\omega}$. While this relationship provides a complete description of reality as far as the permittivities of most real materials are concerned, when relatively small frequency ranges are considered this complex function can be approximated as a single, complex value $\varepsilon^* = \varepsilon' + i\varepsilon''$ where $\varepsilon' = \varepsilon_r\varepsilon_o$, a product of the relative and vacuum permittivities respectively. This expression can be further simplified if the system is taken to be lossless. Since the imaginary term deals with energy loss in a medium, it can be taken to equal zero, thus the complex permittivities of both the particles and the fluid media can be approximated with real values in many situations; say ε_p and ε_f respectively.

When exposed to an electric field of the proper frequency, the particle with permittivity ε_p is polarized and can be represented as a dipole with moment $\boldsymbol{p} = q\boldsymbol{d}$. Here $\boldsymbol{d}$ is the vector distance from the positive end of the dipole to the negative. Its magnitude is d, and this is equal to segment AB in **Figure 3.1**. In working toward a description of the

dielectrophoretic force, it is essential to determine the effect which the particle of given permittivity has on the electric field in which it lies. One may start with obtaining the expression for the potential due to the particle's dipole. The potential due to a dipole is simply the sum of the potentials due to both charges.

$$\varphi = \frac{1}{4\pi\varepsilon_f}\left(\frac{q}{r_1} - \frac{q}{r_2}\right) \tag{1}$$

In order to proceed further it is best to visualize the situation as depicted in **Figure 3.1** below.

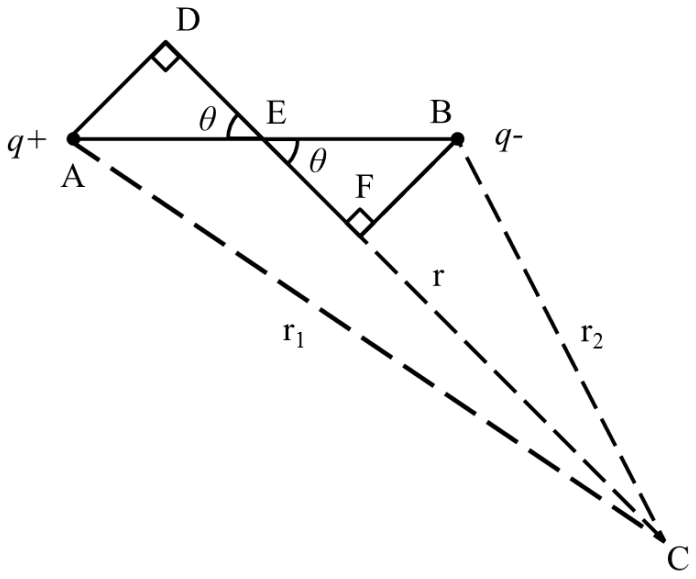

Figure 3.1: Dipole illustration relative to reference point: C

Here it can be seen that r_1 is the distance from the positive dipole to the reference point C and r_2 is the distance from the negative dipole to the reference point. If $r_1 = AC \approx CD = r + \frac{d}{2}\cos(\theta)$ and $r_2 = BC \approx CF = r - \frac{d}{2}\cos(\theta)$, then **Equation 1** can be modified as follows.

$$\varphi = \frac{q}{4\pi\varepsilon_f}\left(\frac{1}{r+\frac{d}{2}\cos(\theta)} - \frac{1}{r-\frac{d}{2}\cos(\theta)}\right) = \frac{q}{4\pi\varepsilon_f}\left(\frac{dcos(\theta)}{r^2-\left(\frac{d}{2}\right)^2\cos^2(\theta)}\right) \quad (2)$$

If r is taken to be much larger than d, then:

$$\varphi = \frac{qd\cos(\theta)}{4\pi\varepsilon_f r^2} \quad (3)$$

Remembering that $|\boldsymbol{p}| = qd$, and since $p\cos(\theta) = \boldsymbol{p}\cdot\hat{\boldsymbol{r}}$, the following substitutions can be made:

$$\varphi = \frac{\boldsymbol{p}\cdot\hat{\boldsymbol{r}}}{4\pi\varepsilon_f r^2} \quad (4)$$

In the above expression, $\boldsymbol{r}$ is the vector distance from the source charge generating the electric field to the center of the dipole, and r is its magnitude. If the particle itself is now considered and assigned a radius r', its physical effect on the surrounding electric field can be expressed as an electrostatic potential. The following relation assumes that the radius r' of the particle is small compared to global field inhomogeneity.[23]

$$\varphi' \approx \frac{(\varepsilon_p-\varepsilon_f)(r\prime)^3\boldsymbol{E}_o\cdot\boldsymbol{r}}{(\varepsilon_p+2\varepsilon_f)r^3} \quad (5)$$

The effective moment is determined by setting these two electrostatic potentials equal to each other and solving for the original dipole moment term.

$$\boldsymbol{p}' = 4\pi\varepsilon_f(r')^3\boldsymbol{E_o}\left(\frac{\varepsilon_p-\varepsilon_f}{\varepsilon_p+2\varepsilon_f}\right) \quad (6)$$

If the permittivities in **Equation 6** are again replaced with their full complex versions, the portion of this equation in parentheses is the Clausius-Mossotti factor, an important relation in determining the principal descriptive equation of dielectrophoretic force.

$$K = \left(\frac{\varepsilon_p^*-\varepsilon_f^*}{\varepsilon_p^*+2\varepsilon_f^*}\right) \quad (7)$$

In moving toward the final derivation of the force on the dielectric particle, it is again important to note that the radius of the particle is small in comparison to field inhomogeneity. This assumption allows for the force on such a dipole to be approximated as follows:

$$\boldsymbol{F} \approx (\boldsymbol{p} \cdot \nabla)\boldsymbol{E_o} \tag{8}$$

When the expression for $\boldsymbol{p}'$ is substituted for $\boldsymbol{p}$ into **Equation 8**, the resulting expression is the force due to dielectrophoresis on the polarized particle. Note that only the real part of the Clausius-Mossotti factor is relevant for the reasons stated earlier.

$$F_{DEP} = 2\pi(r')^3\varepsilon_f \mathrm{Re}\left(\frac{\varepsilon_p^* - \varepsilon_f^*}{\varepsilon_p^* + 2\varepsilon_f^*}\right)\nabla|\boldsymbol{E}_o|^2 \tag{9}$$

It is easy to see from **Equation 9** that if all other terms remain constant, it is the relationship between the permittivities of the particle and the media which determine the sign of the dielectrophoretic force. Specifically if $\varepsilon_p > \varepsilon_f$, then the force will be positive, and the particle will be attracted to regions of higher field strength; if $\varepsilon_f > \varepsilon_p$, it would follow that the sign of the force would be negative, and thus the particle would be repelled from regions with high field strength.

3.2 Role of Other Forces Present

3.2.1 Electrophoresis

Electrophoresis is quite different from dielectrophoresis, though both rely on the interaction of electric fields with particles suspended in media having at least some liquid characteristics. As a brief explanation of this phenomenon, a particle with some net

charge is subjected to a homogenous (spatially uniform) electric field exerting an electrostatic force on the particle itself. Due to the electric double layer effect, an equal in magnitude, yet oppositely charged cloud of ions surrounds the particle (if sufficient ions are in solution) and is forced in the opposite direction by the potential due to a corresponding electrostatic charge, analogous to a boat being paddled against a current.

The drift velocity of a particle undergoing electrophoresis is given by **Equation 10** below.

$$\boldsymbol{v_d} = \mu \boldsymbol{E} \tag{10}$$

Here μ is the particle's mobility, which is proportional to its charge, and $\boldsymbol{E}$ is the electric field. When a particle is in motion at a constant velocity due to electrophoresis, it theoretically experiences no net force. The attractive/repulsive force due to the electric field acting on the particle is balanced by the friction force and the retarding force of the diffuse layer of ions being drawn in the opposite direction. The force on the charged particle due to the electric field is simply:

$$\boldsymbol{F} = \boldsymbol{E}q \tag{11}$$

The friction force and the ionic retarding force are related to the particle size as well as the viscosity and ionic concentration of the solution.

The polystyrene beads used in our studies contained, or more than likely were surrounded by something with a net negative charge (likely sulfate groups left over from the polymerization process), and responded as such when exposed to DC fields in ionic solution by aggregating at the positively charged electrode (when the media was in direct contact with the electrode). This process is somewhat analogous to ionic current with the

charged species too behaving like very large ions. Once the plastic sheet was placed over the electrode, the effects of electrophoresis were no longer observable.

If the beads do indeed have a small negative charge as is demonstrated by performing electrophoresis without the insulating membrane, it would seem that a similar response should be observed even when the LDPE sheet is present. This is not the case even when exorbitantly high DC voltages are applied (>200V). It is possible that this lack of a response is simply due to the increased distance from the charged bead to the electrode surface contributed by the insulating plastic sheet, but with such high voltages, it would seem that there should be significant forces due to electrophoresis if these aspects of the system are indeed properly understood.

3.2.2 Joule Heating and Conductivity

The conductivity of the media is another relevant topic of discussion. When the electrode is in direct contact with the aqueous particle suspension, there is significant risk involved with using very high conductivity media. When the conductivity is relatively high (>0.1 S/m), there are significant flow patterns generated in the media due to joule heating caused by ionic current. When voltages are high enough (>2V_{pp}), electrolysis of the media occurs and can become very violent above 10V_{pp}, causing irreparable damage to the electrode, though usually this is also limited to low frequency signals (<1kHz). As the ionic concentration increases, ionic current increases while at the same time the resistance of the solution decreases. These two relationships oppose each other according

to Joule's First Law (**Equation 12**) the heat generated is proportional to resistance as well as the square of the current.

$$Q \propto I^2 R \tag{12}$$

$$V = IR \tag{13}$$

$$W \sim \sigma E^2 \tag{14}$$

The term Q in **Equation 12** is the resistive heat generated by a current. Due to the fact that there is theoretically a linear relationship between current and resistance (Ohm's Law: **Equation 13**), the current squared term dominates and the heat generated increases with a linear relationship to increasing current.

In addition to these relationships, the power dissipated in the solution is directly proportional to the conductivity and the square of the electric field (**Equation 14**). This work; however, can take the form of not only joule heating, but also AC electro-osmosis, electrophoresis, and dielectrophoresis, as well as any other potential losses to which such a real system would be open. The electric field strength must be significant enough to produce the desired effect of particle arrangement through dielectrophoresis, thus in order to reduce the energy dissipated in the system, it is important to keep the media conductivity low.

It is also important to note that the convective flow initiated in a solution by the application of heat can be quite complex. The force of these flow patterns on particles are observable, but are often quite difficult to quantify in complex systems without modeling software such as COMSOL.

When the conductivity of the media is desirably low, which is about 10^{-5} S/m for DI water, this poses a problem for anyone wishing to manipulate and especially culture bioparticles such as human cells. These cells not only require available ions in their growth media for proper function, they also contain a relatively high concentration of such ions. When cells are kept in low conductivity media, in a dielectrophoresis setup for an extended period of time, they release ions into the solution, thus raising its conductivity and reducing the effectiveness of dielectrophoretic alignment.

The issue with low conductivity could be a problem if cells were to be cultured in our dielectrophoresis setup, but if such long term culture is desired, there is a relatively simple way to solve this problem, though that was not the aim of our studies. It has been demonstrated by Ho, C. et. Al. that if the fluid compartment over the electrodes is designed as a flow chamber with various inlets and outlets for cell suspensions, media of various compositions, etc., the low conductivity dielectrophoresis media can be removed and easily replaced with growth media.[22] This setup also requires that the electrode, or whatever surface on which the cells are to be cultured, must be treated with poly-D lysine to allow the cells to adhere quickly after they are properly aligned so as to prevent them from being washed away by the influx of new media.

While the low conductivity problem could be solved with a few such modifications, the majority of the issues listed above associated with high conductivity media are already completely ameliorated through the design of our setup. Due to the polymer membrane insulating the electrode from the solution, there is little ionic current; therefore there is also minimal electrophoresis. Also if there is such limited current

between the interlocking digits of the electrodes, there is also limited joule heating and therefore negligible electrothermal flow in the media. There is also very little electrolysis observed on the electrode. It is important to note that some electrolysis can occur due to the use of a film of DI water between the electrode and the plastic sheet, but this phenomenon is limited to low frequency (<1kHz) and relatively high voltage (>40Vpp). This frequency range is not useful for performing dielectrophoresis on the particles analyzed in these studies.

While the majority of the issues associated with high conductivity media do not affect this setup, the fact remains that as media conductivity increases, effectiveness of negative dielectrophoretic alignment decreases. Due to the fact that there are no observable signs of the ionic currents or flow patterns due to electrothermal convection usually responsible for disrupting dielectrophoretic alignment, another explanation must be provided for this difficulty. If the system is thoughtfully examined such reasons can be provided and to some extent, tested and validated through experimentation and COMSOL Multiphysics modeling. As far as cells are concerned, the lack of any observable response using high conductivity media could be due to there being insufficient differences between the relative permittivities of the cells and the media. This would prevent the polarization differential necessary for motion in the presence of an inhomogeneous electric field.

It is likely that other processes discussed in this section are occurring, but simply at an almost imperceptible level. It is also likely that when the dielectric particles are polarized in solution, the ions interact with the poles and form a shielding double-layer of

oppositely charged particles. Such a double-layer could theoretically dampen the effect of dielectrophoretic forces as the bead double-layer system would, if taken as a whole, no longer exhibit significant polarization.

One inarguable and significant difference between this setup and those in which the media is allowed to directly contact the electrodes is that current is not allowed to pass directly from one interdigitated electrode through the solution to the corresponding grounded electrode. The electrodes themselves experience little or no current (therefore the function generator theoretically supplies little or no power). The only current is that which is induced in the solution, which is insulated from the electrode (as long as the breakdown voltage of the polyethylene sheet is not exceeded; an issue which is easy to avoid).

3.2.3 AC Electro-osmosis

This phenomenon involves the movement of a diffuse double-layer of charges in a fluid which screens the charge present on electrodes in close proximity to one another. This phenomenon is time dependent in a similar way to the circuit shown in **Figure 3.2** below. The capacitors represent the diffuse double-layer interactions with the electrode surface and the connecting resistors of various lengths (representative of their relative resistances) indicate paths of ionic current through the solution. The paths closer to the gap experience greater electric field and have lower resistance due to their being shorter. Thus the portions of the electrodes which are closer to each other will become shielded faster than areas that are farther away. This DC response elicits induced charge electro-

osmotic flow away from the gap in both horizontal directions. This only occurs briefly in a DC system because such a flow can only be generated when the electrode surface is partially shielded through the interaction between the unshielded region of the electrode surface and the induced charge surrounding the shielded region.

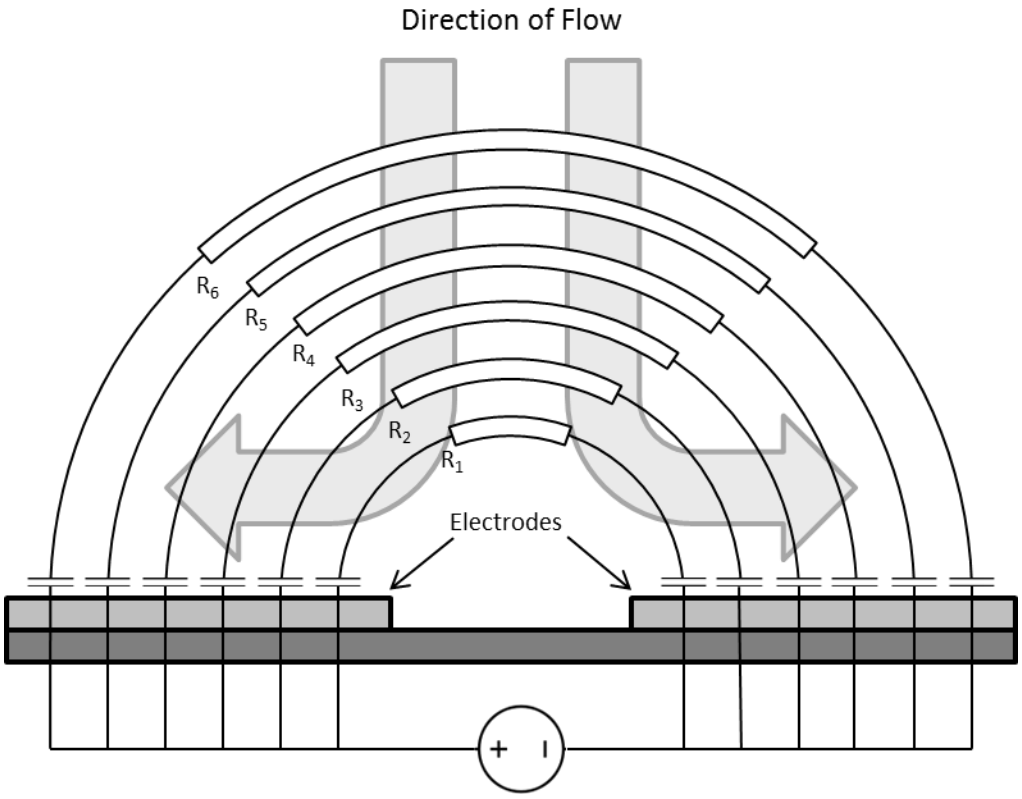

Figure 3.2: Electro-osmosis theoretical circuit diagram

In AC systems, the polarity is reversed, thus inducing another pulse of flow outward from the gap in the same directions as before. This is due to the full reversal of the system; not only is the polarity of the electrodes reversed, so are the charges of the ions attracted to form each diffuse double-layer. The same temporal asymmetry exists in the formation of each double-layer, and it follows that the pattern of flow would also be

the same. For the flow to be relatively continuous, it is essential that the frequency is high enough that the induced shieling layers are not allowed to fully form and low enough such that there is sufficient time for a significant amount of charge to aggregate relative to the scale of the system. The flow rate due to AC electro-osmosis is at its maximum when the period of the field's oscillation is near to the system's time constant.

The fluid velocity due to an applied electric field is largely due to the potential drop across the diffuse layer of ions as it forms over the electrode surface and can be represented by:[8]

$$v_{EO} = \frac{\varepsilon_f}{\eta} \Delta\varphi_d E_t \tag{15}$$

In **Equation 15**, ε_f is the permittivity of the media, η is the dynamic viscosity, φ_d is the potential drop across the diffuse layer, and E_t is the component of the electric field tangent to the electrode surface.

The experimental conditions where the effects of AC electro-osmosis dominate are theoretically limited to lower frequencies than are useful for dielectrophoresis, especially when the conductivity of the media is of a similar magnitude to that of DI water (~10^{-5}S/m). As the conductivity of the media rises to a near physiological level, forces due to AC electro-osmosis increase in strength and may dominate the system in the high kilohertz to low megahertz range (along with electrothermal flow patterns).[8] This relationship makes intuitive sense due to the fact that as the conductivity of the solutions increases, there are more ions available to form shielding double-layers at the electrode fluid interface.

3.2.4 Brownian Motion

This is the random motion of particles suspended in a fluid due to their encounters with the randomly moving atoms and/or molecules of which the fluid consists. The extent of the motion due to this process in a fluid system with a low Reynolds number can be derived by staring with the Stokes-Einstein equation.

$$D = \frac{k_B T}{6\pi\eta r} \tag{16}$$

This relation describes the diffusion constant *D* in term of the temperature *T*, the Boltzmann's constant k_B, the fluid's viscosity η, and the radius of the spherical particle *r*. The Stokes-Einstein equation serves as the basis for the equation show below describing the one dimensional motion of a particle due to Brownian motion as a function of time *t*.

$$X_B(t) = \sqrt{\frac{k_B T}{3\pi\eta r} t} \tag{17}$$

For particles as large as cells, Brownian motion is nearly irrelevant when its effects are compared to those of the other forces listed in this section. If the particles are very small (< 1μm in diameter), then Brownian motion has a more significant effect as long as the forces generated by the other phenomena listed above are suitably small as in systems with low frequency, low voltage, and very high conductivity. The small size of the contribution of Brownian motion to the overall motion of a particle in a system used for dielectrophoresis can be easily seen from **Equation 17** above and is due to the size of the Boltzmann's constant (~1.38×10^{-23}J/K).

The 2μm polystyrene beads used in some of our studies experience this phenomenon to the largest extent. Their mass is sufficiently small for Brownian motion

to contribute significantly to their overall motion when the applied dielectrophoretic force is sufficiently small. This means that smaller beads such as these, or indeed any small particles, will tend to lose their alignment faster after electric fields are removed.

CHAPTER FOUR

EXPERIMENTATAL SETUP DESIGN

4.1 Introduction

The chief design objective is to create a low voltage/low power system for moving and aligning particles (polystyrene beads and cells) using dielectrophoresis. Such a setup should theoretically minimize the interfering effects of the other forces discussed in the previous chapter. This was done in several experimental steps. First traditional direct media-electrode contact dielectrophoresis was attempted. Then a setup was constructed using a 12.7μm thick sheet of LDPE to separate the particle suspension from the electrode. In the final setup, the electrode was coated with a 4μm thick layer of SU-8 photoresist. For all of these setups microfabricated electrodes were required, and were fabricated using masks of the shapes pictured below and following the procedure outlined in this chapter.

4.2 Electrode Mask Geometries

Three basic electrode geometries are used for various elements of these studies: straight interdigitated **Figure 4.1**, square interdigitated **Figure 4.2**, and round interdigitated **Figure 4.3**. Three different sizes (variations in electrode width and spacing) of straight interdigitated electrodes and two different square electrodes are used for various purposes, thus giving a grand total of six different electrode geometries. The digit width and spacing are similar in each of our designs and range from 10-120μm. The three

pictured below are not necessarily to scale and are simply intended to represent the basic shapes of electrode mentioned above.

Note that the large rectangles on either side of the interdigitations are the contacts where copper tape was applied. If the setup was coated with SU-8, these areas would be masked so that none of the photoresist would adhere in order to allow the electrode to be connected to the DC power supply or function generator.

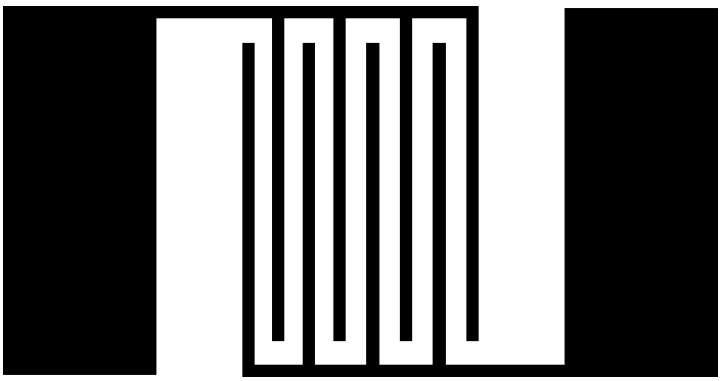

Figure 4.1: Straight interdigitated electrode

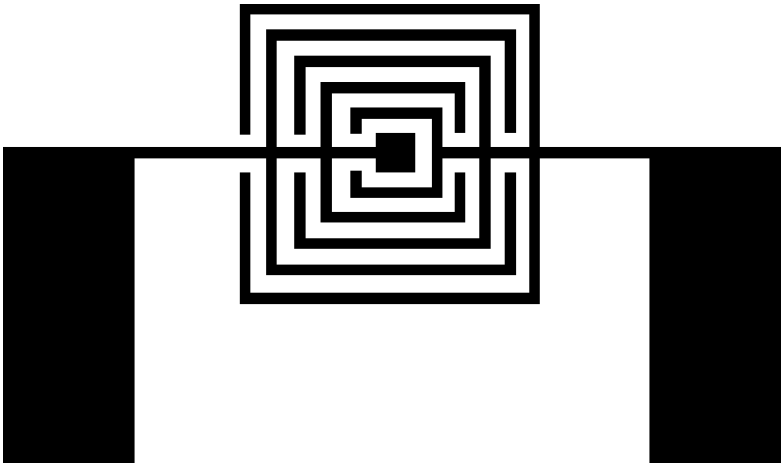

Figure 4.2: Square interdigitated electrode

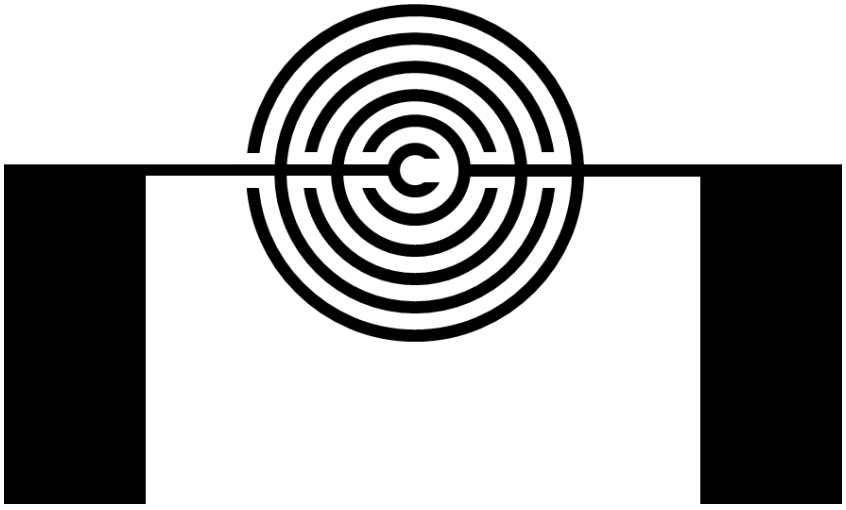

Figure 4.3: Round interdigitated electrode

4.3 Electrode Fabrication Process

4.3.1 Materials for Electrode Fabrication:

1. Glass slides coated with ~20nm layer of Ti under ~100nm of Au
2. Microposit S1818 Positive Photoresist
3. MF-319 Microposit Developer
4. Microposit Remover 1165
5. MCC Primer
6. Acetone
7. Ethanol
8. DI water
9. Patterned mask
10. Model WS-400B-6NPP/Lite Spin Coater
11. Karl Suss Mask Aligner/Mimir Model 505 Optical Energy Controller

12. Harrick Plasma Plasmaflo Plasma Cleaner/Sterilizer
13. Fisher Scientific FS30D Ultrasonic Cleaner
14. Barnstead Thermolyne SUPERNOVA Hotplate
15. Potassium Iodide
16. Iodine
17. Hydrofluoric Acid
18. Hydrogen Peroxide

4.3.2 Procedure for Electrode Fabrication:

Thoroughly clean the Ti/Au coated glass slide by first ultrasonicating it in ethanol for five minutes and rinsing thoroughly with DI water. Then blow dry with compressed air. Next place the glass slide in the oxygen plasma chamber and follow the plasma cleaning procedure outlined immediately following this section.

Once this process is complete, place the cleaned slide onto the spinner pedestal, metal side up, and fix it in place with the vacuum. Program the spinner to use the following three step process for all runs. The first step should be at 1000rpm for 30 seconds, the second step is 3000rpm for 30 seconds, and the final step is again 1000rpm for 30 seconds. Once the program is set rinse the gold with acetone while it is attached to the spinner. Run the spinner program to fully remove the acetone. Next completely coat the metal surface of the slide with the primer and once again run the same spinner program. When this step is complete, apply an even coating of S1818 photoresist to the gold being careful not to actually touch the delicate metal surface. Quickly run the

program one last time to achieve a 2μm thick coating of photoresist. The next step involves baking the coated electrode at 90°C for 10 minutes uncovered on a hotplate in order to remove any solvent left in the photoresist coating.

Once the photoresist is sufficiently dry the actual lithography process can begin. This involves carefully positioning the mask over the photoresist and making sure that there is hard contact between the mask and the photoresist. It is then exposed to a ~200mJ/cm^2 UV lamp for one minute. The sample is then immediately submerged in MF-319 developer solution and agitated until only the appropriate areas remain masked. It is important to then rinse the sample in DI water and dry it thoroughly before the final hard bake procedure. This final baking should be at 120°C for 10 minutes.

Now that the electrode area has been appropriately protected with the photoresist coating, the process of etching away the unwanted gold and titanium can begin. The gold must be removed first as it is the topmost layer. This involves submerging the electrode in a solution of 4g KI and 1g I_2 dissolved in 40mL of DI water for 30-40 seconds, then rinsing it with DI water and drying it thoroughly before moving on to the titanium removal step. The titanium etchant is a 1:1:20 solution of H_2O_2, HF, and DI water respectively. The sample is dipped in this solution for 10-15 seconds or until the regions of glass not coated with photoresist become clear.

After again rinsing and drying the electrode, it is time to remove the protective photoresist. This can be accomplished by soaking the sample in a bath of either Microposit Remover 1165 or Acetone until no more of the red photoresist is visible. This step is followed by an additional five minute ultrasonic cleaning in ethanol to make sure

that all photoresist material has been removed. The finished electrode is then rinsed and dried one final time before it may be used.

4.3.3 Plasma Cleaning Procedure:

Once a metal coated sample has been subjected to ultrasonic cleaning, thoroughly rinsed, and dried; it must be further cleaned with oxygen plasma before it can be coated with photoresist for patterning. First check that the three way valve on the plasma chamber is in the closed position. Also check that the flowmeter valves are closed. Then put the sample in the plasma chamber, close the door, and turn on the PlasmaFlo main power. Turn on the vacuum pump. The pump will hold the door of the plasma chamber closed. Pump the chamber down to ~200mTorr before bleeding in the oxygen. In order to add the oxygen to the chamber, first turn the plasma chamber valve so that it is pointing to the left. Allow the pressure to equilibrate back to ~200mTorr. Then open the valves on the oxygen cylinder. Be sure that the regulator valve is set to 10psig. Slowly open the regulator isolation valve. Now slowly open the flowmeter valves until the flow level reads 10mm on the reference scale.

Now turn on the Plasma Cleaner main power. Slowly step the RF power level from low to medium to high. A violet plasma should be observed in the chamber, if the plasma is blue, then the chamber still contains air (as opposed to oxygen). It is important that the process of purging the chamber of air be repeated properly before the cleaning process can continue. If the plasma is the appropriate color, then the sample should be left in the chamber at high RF power for two minutes.

After this time has passed turn off the RF power. Then turn off the plasma cleaner main power. Close all valves on the oxygen cylinder and close the isolation valve. Allow the pump to run for 1-3 minutes to remove any residual oxygen. Next close the flowmeter valve. Turn off the pump and slowly rotate the three way valve into the upright position. This breaks the vacuum in the chamber. Once the pressure in the chamber has reached equilibrium with that in the room, the chamber can be opened and the sample removed.

4.4 Experimental Setups

Once the electrodes were fabricated, they were used in one of the following three types of setup. These are ordered in the sequence that they were developed, and in order of decreasing power dissipation.

4.4.1 Direct Media-Electrode Contact:

This setup is the most basic and relatively similar ones have been in use since the phenomenon of dielectrophoresis was first subjected to serious study. It simply consists of an electrode (in this case a photolithographically patterned planar interdigitated electrode) indirect contact with a particle suspension within a small fluid chamber.

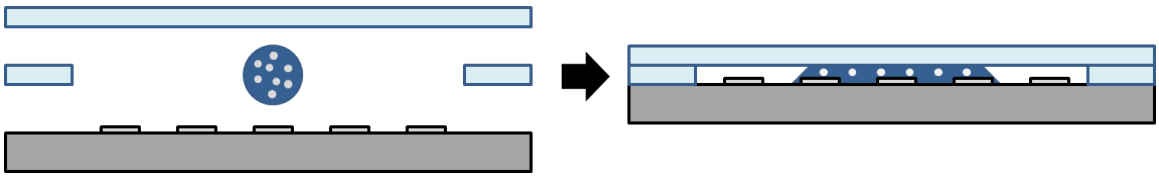

Figure 4.4: Direct media-electrode contact setup

In this particular setup, depicted in **Figure 4.4**, the media is of widely varying conductivity adjusted by the addition of KCl or NaCl. The fluid chamber is very simple and consists of 100µm thick glass spacers supporting a glass coverslip of identical thickness.

For all setups, AC potentials are applied with a Wavetek Model 190 20MHz function generator, which has the frequency and potential ranges of 0-20MHz and 0-32Vpp respectively. These signals were monitored with a Tektronix TDS 1001C-EDU oscilloscope. The DC potentials were supple by an Agilent Technologies N5751A System DC Power Supply.

4.4.2 Protective LDPE Sheet

The addition of the LDPE sheet (which is simply Great Value sandwich wrap) greatly added to the reliability of dielectrophoretic alignment. The setup is very similar to the one described above except for the added plastic sheet as shown in **Figure 4.2** below.

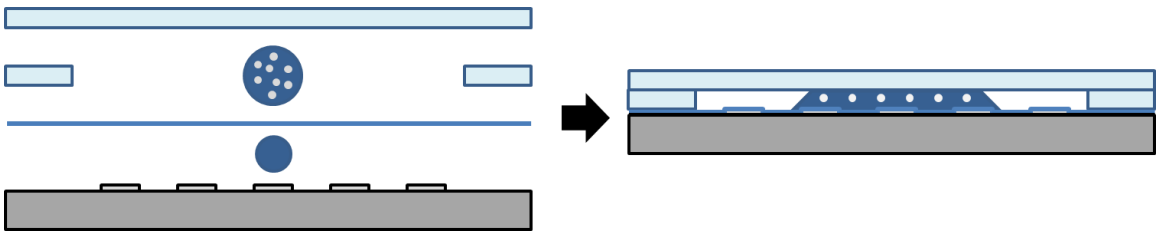

Figure 4.5: LDPE sheet setup

The blue line in **Figure 4.5** represents the ~12μm thick LDPE sheet, and the dark blue circle immediately below the plastic sheet represents a drop of DI water that is added only to provide better physical contact between the electrode and the LDPE sheet. It is demonstrated in the studies to be detailed later that whether or not this drop is present has little effect on the magnitude of the dielectrophoretic force.

4.4.3 SU-8 Coated Setup

The construction of this setup required an additional photolithographic fabrication step; its description is as follows:

4.4.3.1 Materials for SU-8 Coating:

1. Patterned Electrode
2. Mask Covering Electrode Contacts
3. SU-8 2005 Negative Photoresist
4. SU-8 Developer
5. Acetone
6. Ethanol
7. DI Water
8. Model WS-400B-6NPP/Lite Spin Coater
9. Karl Suss Mask Aligner/Mimir Model 505 Optical Energy Controller
10. Fisher Scientific FS30D Ultrasonic Cleaner
11. Barnstead Thermolyne SUPERNOVA Hotplate

4.4.3.2 Procedure for SU-8 Coating:

The patterned electrode must first be ultrasonicated for five minutes to clean it and then rinsed with DI water and blown dry. Place the cleaned electrode on the spinner pedestal and fix it in place with the vacuum. The spinning times and speeds are the same as those used for S1818, and are as follows: 30 seconds at 1000rpm, 30 seconds at 3000rpm, and a further 30 seconds at 1000rpm. Once this program is set, rinse the sample thoroughly with acetone and use it to spin the sample dry.

The electrode is now ready to be coated, and should be carefully covered with SU-8 2005, making sure not to touch the electrode surface when applying the polymer. The three step spinning program should now be run. Immediately after the spinning step is complete, the electrode should be transferred to the hot plate where it is to be baked at 65°C for 3 minutes, uncovered.

Exposure times and intensities for this procedure are the same as for S1818 and are as follows: one minute at ~200mJ/cm^2. Once the electrode has been exposed it must be baked on the hotplate again for 3 minutes at 95°C before being submerged in developer and agitated for one minute or unit the photoresist has been removed from the masked areas, which in this case should be the contacts where copper tape will be placed for attachment to the function generator. Thoroughly rinse the coated electrode with DI water and blow it dry. The final step is a hard bake; set the hotplate to 95°C, then ramp the temperature up to 200°C and hold this temperature for 10 minutes. Ramp the temperature back down to 95°C before removing the electrode from the hotplate and allowing it to assume room temperature.

The setup is then assembled exactly the same way as if the electrode were uncoated, with glass spacers and a glass coverslip forming the fluid chamber and viewing area above the insulated electrode digits. This is the most protected electrode setup; the SU-8 coating is very durable even though it is scarcely 4µm thick as confirmed by ellipsometric testing. A schematic of this setup is shown in **Figure 4.6**.

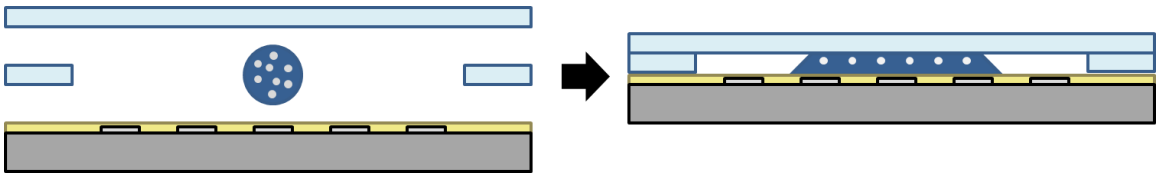

Figure 4.6: SU-8 coated setup

The yellow rectangle represents the SU-8 coating, which is in reality nearly as flat a surface as is depicted here. Atomic force microscopy studies have shown that while the metal digits of the electrode are ~120nm thick, after they are coated, the variation in height from the gap between electrodes to the center of an electrode digit is ~10nm.

CHAPTER FIVE

STUDIES WITH DIRECT MEDIA-ELECTRODE CONTACT

5.1 DC Testing With Direct Media Contact

5.1.1 Purpose:

The reason for performing these studies is to determine whether or not there is significant charge on the polystyrene beads so that a more complete picture of the physical parameters of the beads is available for modeling and understanding potential outcomes of future studies. The results of this study are also meant to be compared with those of similar studies to be described later in which the media containing polystyrene beads is isolated from the electrode by some type of polymer coating.

5.1.2 Materials for DC Testing With Direct Media Contact:

1. Patterned Electrode
2. Glass Slide
3. Glass Spacers
4. Glass Coverslip
5. Copper Tape
6. 4.5µm Diameter Polystyrene Microspheres (Polysciences, Inc. Polybead®)
7. DI water
8. KCl
9. Agilent Technologies N5751A System DC Power Supply

10. Tektronix TDS 1001C-EDU Oscilloscope
11. ZEISS Axiovert® S100 Inverted Microscope
12. JENOPTIC ProgRes® Speed XT Core 3 Camera
13. JENOPTIC ProgRes® CapturePro 2.8 Software

5.1.3 Methods for DC Testing With Direct Media Contact:

The electrode is attached to a glass slide with double sided tape so that it can be secured in the slide bracket on the inverted microscope. Two pieces of copper tape are cut measuring about 3cm × 0.5cm and are adhered to the contact pads of the electrode. Two 1:10 dilutions of the original bead suspension were performed with DI water and 1mM KCl. A 20µL aliquot of bead suspension is placed within the setup corresponding to **Figure 4.4**, attached to the power supply, and secured in the slide bracket on the inverted microscope.

The power supply is then set to 0V DC and turned on. The voltage is slowly ramped up until there is a noticeable response from the beads in solution. If such a response takes place, then there is a note made of the voltage at which the beads respond. The oscilloscope was used to monitor the voltage levels and to make sure that the signal had minimal AC characteristics (usually as a result of high frequency noise if present).

5.1.4 Results for DC Testing With Direct Media Contact:

It was observed that the beads in DI water moved toward and aggregated at the electrode with the more positive voltage as shown in **Figure 5.1**. Interestingly this motion

was not linear, in that they were not immediately attracted to the positive electrode. At lower voltages (2-3V) they began moving toward the negative electrode. As the voltage was increased, they changed direction and aggregated at the positive electrode at 3.3V, making no other movements until electrolysis began at 3.5V. Just as a further test the relative potentials of the electrodes were switched once the beads aggregated at the positive electrode. The beads behaved as expected and quickly dissociated from the electrode on which they were currently aligned and aggregated at the new positive electrode.

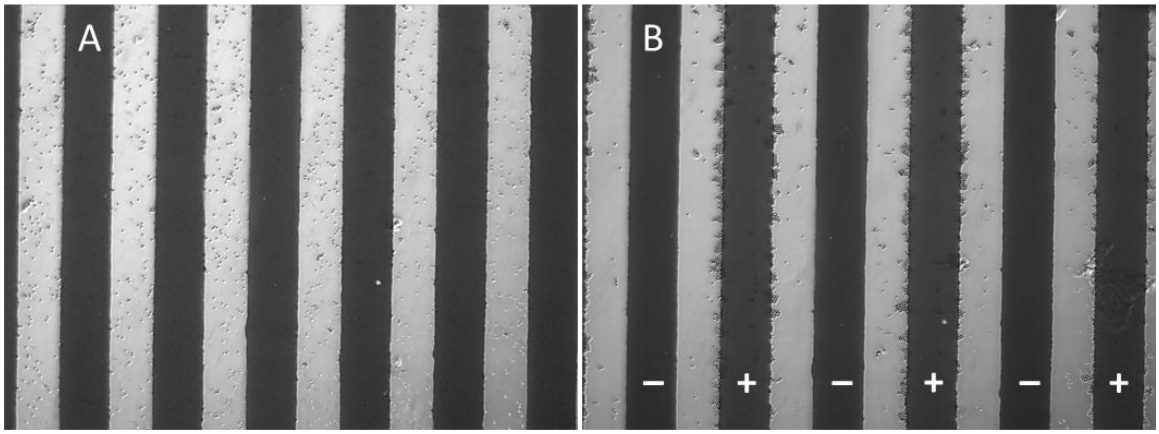

Figure 5.1: 4.5µm polystyrene beads at 0V DC (A) and 3.4V DC (B) in DI water

In the 1mM KCl solution, the beads behaved similarly. There was some nonlinearity to their overall displacement in the direction of the positive electrode, but the beads did aggregate at the positive electrode as shown this time on the circular interdigitated electrode in **Figure 5.2**.

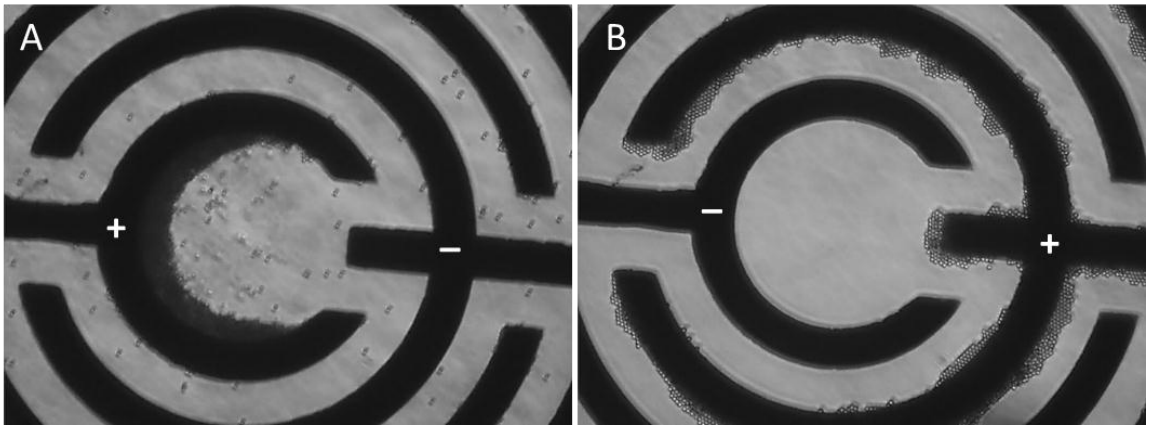

Figure 5.2: 4.5μm polystyrene beads at 3V DC switching polarization in 1mM KCl

This image shows the change in aggregation when the polarity of the electrodes was reversed, a phenomenon which also took place in 1mM KCl.

5.1.5 Conclusions:

The reasons for the nonlinearity in the bead motion at low voltage are likely joule heating and some mild electrolysis eliciting flow patterns in the media. Overall the hypothesis that the beads exhibited an overall negative charge was supported by the results. This electrophoresis was effective in both DI water and ionic solution (1mM KCl).

5.2 AC Testing with Direct Media Contact

5.2.1 Purpose:

These studies are the first attempts made to achieve dielectrophoretic alignment of the polystyrene beads. This started as merely an attempt to replicate the results of others, though the results were not completely as expected.

5.2.2 Materials for AC Testing with Direct Media Contact:

1. Patterned Electrode
2. Glass Slide
3. Glass Spacers
4. Glass Coverslip
5. Copper Tape
6. Double Sided Tape
7. 2µm Diameter Polystyrene Microspheres (Polysciences, Inc. Polybead®)
8. 4.5µm Diameter Polystyrene Microspheres (Polysciences, Inc. Polybead®)
9. 15µm Diameter Polystyrene Microspheres (Polysciences, Inc. Polybead®)
10. DI water
11. KCl
12. Wavetek Model 190 20MHz Function Generator
13. Tektronix TDS 1001C-EDU Oscilloscope
14. ZEISS Axiovert® S100 Inverted Microscope
15. JENOPTIC ProgRes® Speed XT Core 3 Camera

16. JENOPTIC ProgRes® CapturePro 2.8 Software

5.2.3 Methods for AC Testing with Direct Media Contact:

The electrode is affixed to a glass slide with double sided tape and the appropriate components are then arranged as the setup in **Figure 4.4** depicts. Two pieces of copper tape measuring about 3cm × 0.5cm are attached to the contact pads of the electrode and connected to the function generator. The oscilloscope is also connected at this time for monitoring the magnitudes and frequencies of the applied signals.

The frequency and voltage were both varied systematically until a response was observed. The ranges for this variation were 20kHz-20MHz and 0Vpp-32Vpp for frequency and voltage respectively. This process was performed with beads suspended in both DI water and 1mM KCl.

Results:

There was little or no response at all when using DI water at any frequency-voltage combination. At higher voltages, about 5% of the beads would levitate off of the electrode. These beads that levitated were usually between the electrode digits. Some of the beads also lined up along the center of the electrode digits, but this response too was minimal. These subtle phenomena are depicted below in **Figure 5.3**. The circles highlight levitated beads, while the rectangles highlight bead alignment on the electrode digit.

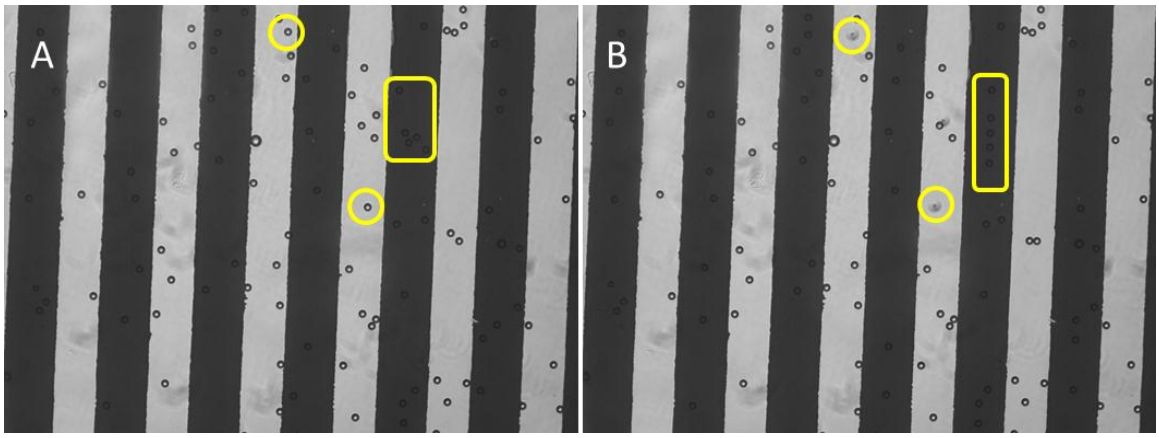

Figure 5.3: 15µm beads at 1MHz 1Vpp (A) and 5Vpp (B) in DI water

When using 1mM KCl, there was a significant difference in bead behavior. Not only did the beads move, but they never completely stopped moving. This could be due to currents from electrothermal activity or from electrolysis of the media. It is even possible that electro-osmosis could have played a role here. For both bead sizes, there was a certain frequency at which they seemed to "resonate" best and group between the electrode digits. This phenomenon is shown in **Figure 5.4** below.

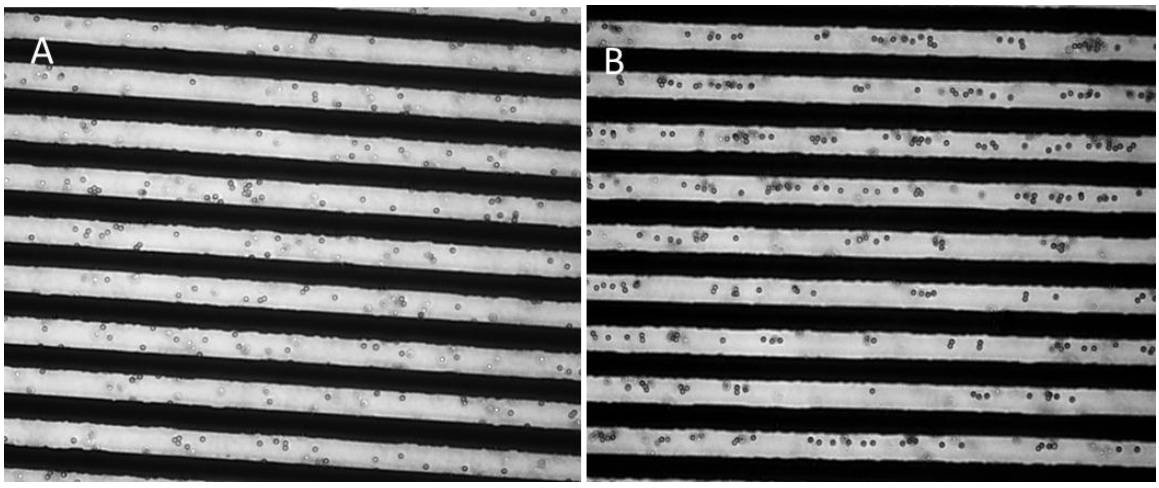

Figure 5.4: 2µm beads 0Vpp (A) and 18.6Vpp 314 kHz (B) in 1mM KCl

The 2µm beads lined up in this way with the greatest reliability at ~300kHz, and the 4.5µm diameter beads lined up at ~30kHz. As a rule the order and density of these lines increased with increasing voltage as can be seen in **Figure 5.5**.

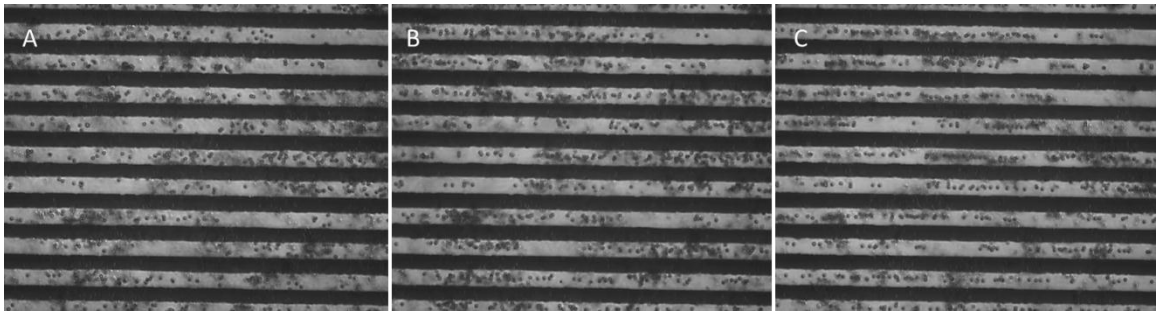

Figure 5.5: 2µm beads at 314kHz, 8Vpp (A) 16Vpp (B) 24Vpp (C) in 1mM KCl

If the voltage was set sufficiently high, 18Vpp for example, and the frequency was swept upward from 20kHz the beads initially moved only randomly. As the signal frequency began to approach the system's resonant frequency the beads would begin to vibrate in the spaces between the electrode digits. Their motion would be perpendicular to the long axis of the digits. The speed of the vibration would increase until the beads appeared almost stationary and were held in place between the electrode digits. It is possible that the behavior could be dielectrophoretic in nature, but it seems to resemble something close to very fast AC electrophoresis.

Conclusions:

These studies did not produce the expected results. There have been a myriad other studies which have achieved obvious positive and negative dielectrophoresis using direct media-electrode contact setups. In fact this is by far the most frequently performed type of dielectrophoresis.

Our results point to there being little dielectrophoresis actually occurring in these setups. It is well documented that low conductivity media (DI water when possible) is best for performing dielectrophoresis. Our studies in DI water demonstrated little or no action which could be called dielectrophoresis. The studies in 1mM KCl did produce particle alignment similar to negative dielectrophoresis, but there was no pearl chain formation, and the entire system was violently active with too many other forces to isolate anything exclusively dielectrophoretic.

CHAPTER SIX

FREQUENCY CHARACTERIZATION OF LDPE SHEET SETUP

6.1 Frequency Sweep with LDPE Sheet

6.1.1 Purpose:

These studies are conducted in order to see if it is possible to achieve dielectrophoretic alignment of polystyrene beads using an electrode insulated from the solution with potentials lower than 32Vpp. The reason for having this goal is to produce a setup in which the electrode is reusable and protected from the particle suspension. A further reason to pursue this goal is to limit the power potentially dissipated in the setup. Other insulated electrode setups utilize a much thicker insulating layer and see significant power dissipation in the water layer present between the electrode and the insulating membrane.

The frequency sweeps directly allow for the behavior of polystyrene beads in the insulated electrode setup to be analyzed over a range of frequencies and bead sizes. These findings are then used to produce refined finite element models using COMSOL Multiphysics software.

6.1.2 Materials for Frequency Sweep with LDPE Sheet:

1. Patterned Electrode
2. Glass Slide
3. Glass Spacers
4. Glass Coverslip

5. LDPE Sheet
6. Copper Tape
7. Double Sided Tape
8. 2μm Diameter Polystyrene Microspheres (Polysciences, Inc. Polybead®)
9. 4.5μm Diameter Polystyrene Microspheres (Polysciences, Inc. Polybead®)
10. 10μm Diameter Polystyrene Microspheres (Polysciences, Inc. Polybead®)
11. DI water
12. Wavetek Model 190 20MHz Function Generator
13. Tektronix TDS 1001C-EDU Oscilloscope
14. ZEISS Axiovert® S100 Inverted Microscope
15. JENOPTIC ProgRes® Speed XT Core 3 Camera
16. JENOPTIC ProgRes® CapturePro 2.8 Software

6.1.3 Methods for Frequency Sweep with LDPE Sheet:
High Voltage Large Electrode Geometry

An interdigitated electrode with 110μm spacing and digit width is attached to the glass slide using double sided tape. Pieces of copper tape measuring about 3cm × 0.5 cm are then attached to the contact pads of the electrode. The experimental setup is then assembled as shown in **Figure 4.5** using one of the three sizes of beads (2μm, 4.5μm, and 10μm diameters). This entire process is repeated for each bead size so as to get a basic idea of the impact of bead size on the frequency response.

The setup is then placed in the slide clip on the stage of the inverted microscope. For the first sweep the magnitude of the AC voltage is held constant at 32Vpp as the frequency is swept from 20kHz to 20MHz. The frequencies where images were obtained are listed in the following table.

Range 1	20kHz-200kHz in 10kHz increments
Range 2	225kHz-2MHz in 25kHz increments
Range 3	2.5MHz to 5MHz in 500kHz increments
Range 4	6MHz to 20MHz in 1MHz increments

Figure 6.1: Ranges for Frequency Sweep

6.1.4 Methods for Frequency Sweep with LDPE Sheet:
High Voltage Small Electrode Geometry

An interdigitated electrode with 50μm spacing and digit width is attached to the glass slide using double sided tape. A piece of copper tape measuring about 3cm × 0.5 cm is then attached to each of the contact pads on the smaller electrode.

Using the same three bead sizes and a voltage of magnitude 32Vpp held constant, the frequency sweep is again performed. Pictures of the bead response are taken at the frequencies listed in **Figure 6.1**.

6.1.5 Methods for Frequency Sweep with LDPE Sheet:
Low Voltage Large Electrode Geometry

The interdigitated electrode with 110μm spacing and digit width was attached to a glass slide. Two pieces of copper tape measuring 3cm × 0.5cm were cut and attached to the contact pads of this electrode. The experimental setup shown in **Figure 4.5** is then constructed using this electrode and one of the three bead sizes.

The frequency sweep process is then performed with the magnitude of the applied AC voltage held at a constant 16Vpp. This process is repeated for each of the three bead sizes and pictures of the beads' behavior are taken at the frequencies listed in **Figure 6.1**.

Thus after all three bead sizes are tested according to each of these three methods; there are a total of nine different sets of frequency sweep data.

6.1.6 Results for Frequency Sweep with LDPE Sheet: High Voltage Large Electrode Geometry

At the lower end of the frequency spectrum, below 20kHz, there were no images obtained despite the 2μm beads already exhibiting rudimentary alignment at 20kHz when using the small interdigitated electrode.

For the first study (large electrode spacing, 32Vpp frequency sweep), the 2μm beads first began to aggregate in the spaces between electrode digits at 80kHz. This loose aggregation became more refined until it exhibited clear pearl chain formation at 100kHz. As the frequency rose, the pearl chains became increasingly well defined. Pearl chain formation peaked at 190kHz and the chains remained straight and with definite separation until about 425kHz. It was from this point that the chains became less straight and the spacing between them decreased. Significant breakup of the pearl chains began at 550kHz and continued until the aggregation between the electrode digits became almost completely random at about 1.15MHz, yet there was still definite aggregation. This dissolution continued until at around 1.875MHz the total distribution of particles over the electrode surface again became completely random with no observable signs of

dielectrophoretic alignment. This random distribution persisted until the study was terminated at 20MHz.

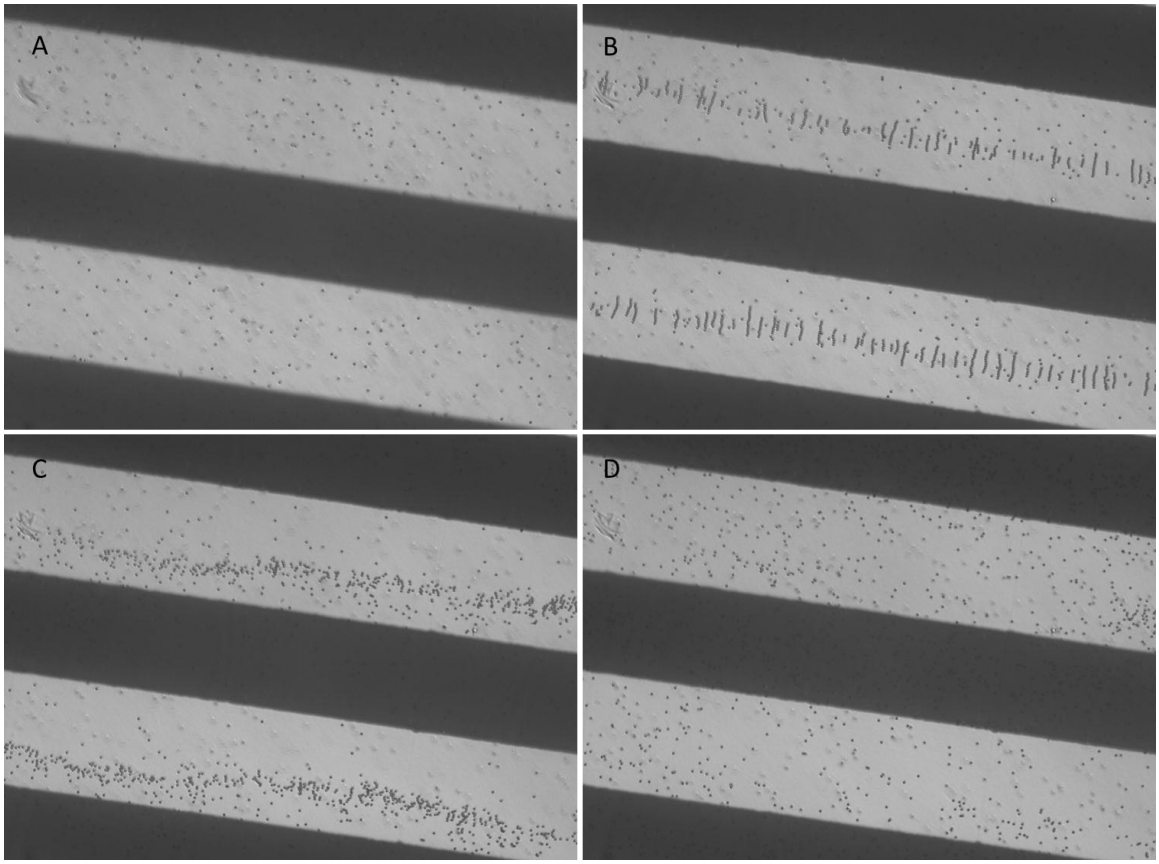

Figure 6.2: 2µm beads, 110µm electrode;
no potential (A), 190kHz (B), 1.15MHz (C), 1.875MHz (D)

The 4.5µm beads first began an observable response to the time varying electric field at 20kHz, but this response was still quite disorganized. Loose aggregations of beads began to form between the electrode digits at around 70kHz before relatively well defined pearl chains formed at 100kHz. The pearl chains were stable until about 300kHz when some of the beads began to lift off of the surface of the LDPE sheet. While many of

the beads kept their pearl chain alignment, the majority of them drifted away from the space between the electrodes. This resulted in a nearly random distribution of pearl chains dispersed high in the solution. Some were able to remain between the electrodes when floating at this height, but if there was any flow present, they were dislodged from their preferred place between the electrode digits.

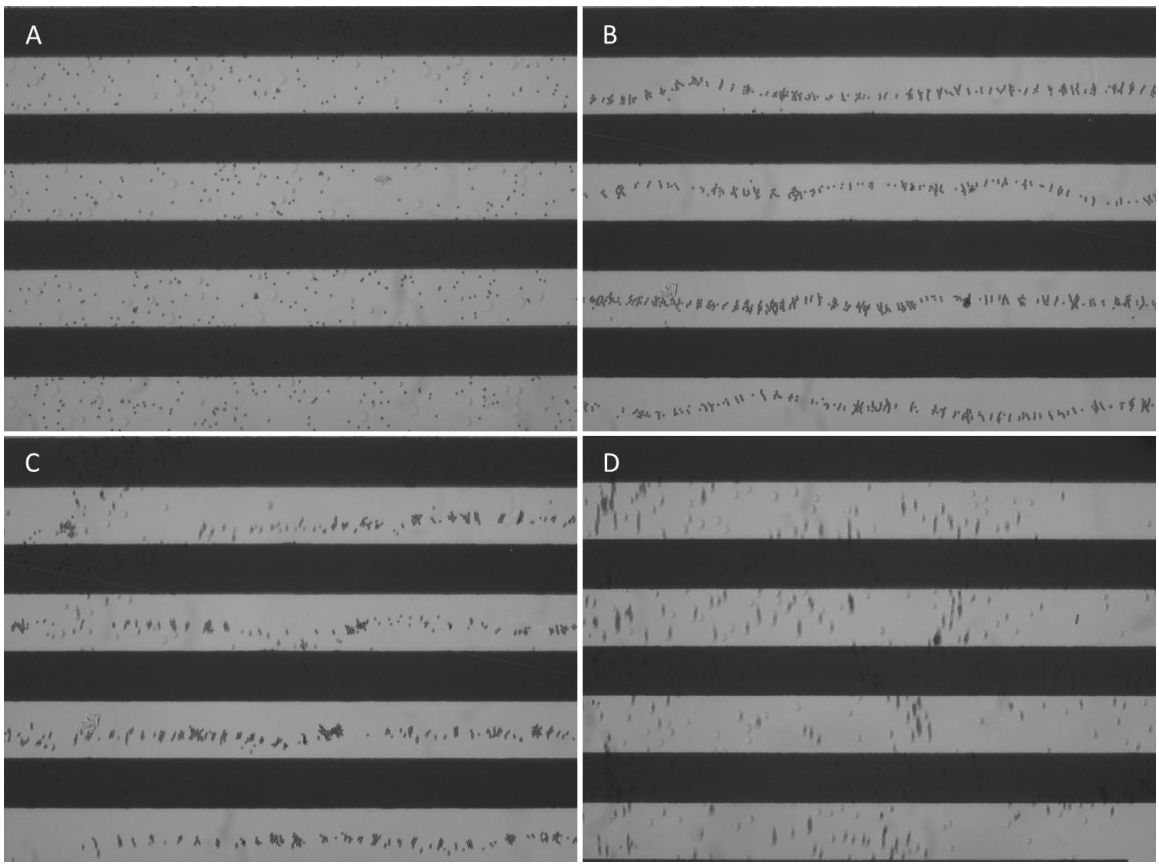

Figure 6.3: 4.5µm beads, 110µm electrode;
no potential (A), 170kHz (B), 425kHz (C), 1.25MHz (D)

For 10µm beads, the results were relatively similar, though there were some differences due to the bead size. Pearl chain formations began as low as 80kHz, but were

not aligned well between the electrode digits until 250kHz. From this point the pearl chains became increasingly well aligned and were very well organized by 300kHz. Some of the chains began to lift off of the LDPE surface at 650kHz, and this process continued until almost all of the chains had lifted. As some of these chains slowly drifted into the space over the electrode, it was observed that they tilted upward and stood on end forming columns of beads over the electrode surface. Upon further examination it was observed that this column formation also occurred with the 4.5µm microspheres, though it was much more obvious with these larger beads. The pearl chains remained off the substrate and together as the frequency sweep continued up to 20MHz.

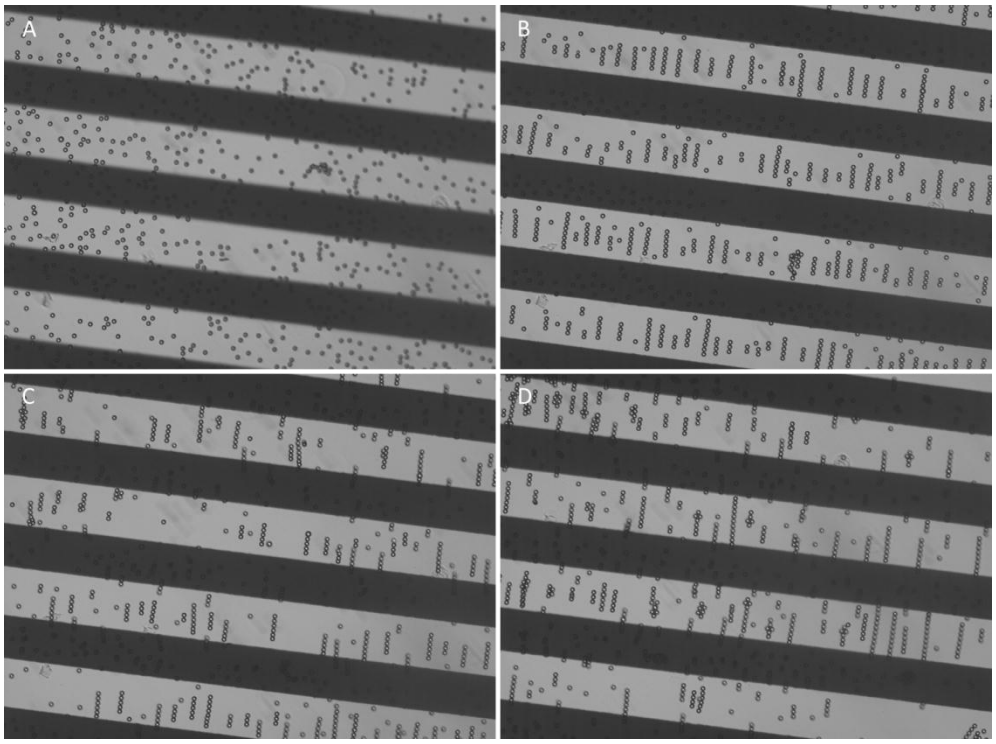

Figure 6.4: 10µm beads, 110µm electrode;
no potential (A), 300kHz (B), 800kHz (C), 1.3MHz (D)

In some tests the pearl chains were dislodged from the spaces between the electrodes by flow patterns present in the solution. These flow patterns were unidirectional.

6.1.7 Results for Frequency Sweep with LDPE Sheet: High Voltage Small Electrode Geometry

It was observed that when using the 50μm electrode, 2μm diameter beads began to align between the electrode digits at 20kHz (the first frequency tested); though at this frequency there was minimal pearl chain formation. There was significant pearl chain formation by the time the frequency was raised to 50kHz. These pearl chains lengthened and became more defined until about 275kHz. At this point the chains began to be pushed harder toward the center of the space between the electrodes. This caused them to become shorter and closer together. The beads then began to lift off of the LDPE surface at about 475kHz. They were unable to maintain their pearl chain alignment, but remained suspended roughly above the space between electrode digits until about 600kHz. At this point the loose aggregations of beads began to move into the space directly above the electrode digits. This loose grouping above the electrode was most evident at 800kHz. After this point the microspheres were almost completely lifted off of the electrode surface and became increasingly random in their distribution.

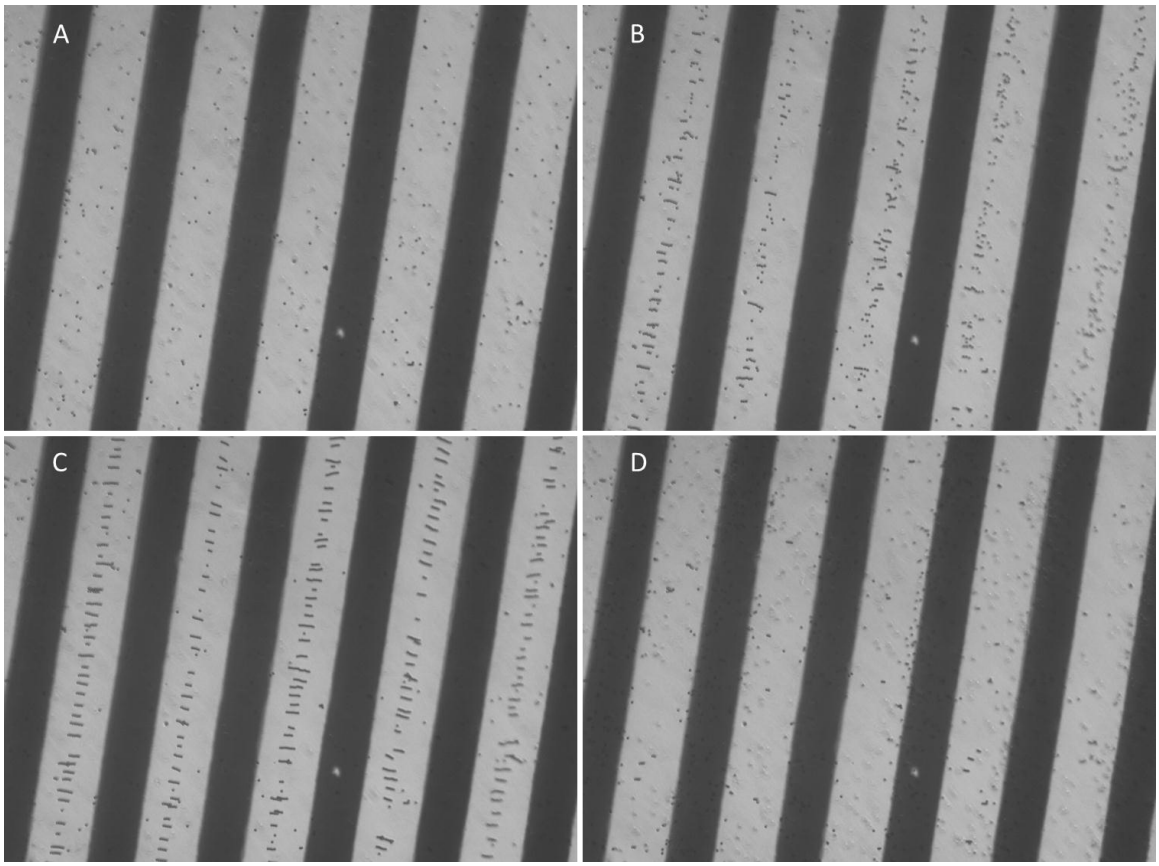

Figure 6.5: 2µm beads, 50µm electrode;
no potential (A), 50kHz (B), 150kHz (C), 800kHz (D)

The 4.5µm diameter microspheres were observed to occasionally exhibit what appeared to be positive dielectrophoresis at frequencies below 100kHz in that they aggregated at the electrode edges where the field was strongest. This transitioned to clearly negative dielectrophoresis by 150kHz, though no pearl chains had yet formed. Pearl chains formed around 275kHz, but the beads were already being lifted and drifting out of the spaces between the electrode digits. In some frequency sweeps, the beads appeared to exhibit something resembling positive dielectrophoresis again at about 400kHz. Pearl chain formation continued until the end of the frequency sweep, though

the beads remained up off of the electrode surface. When the pearl chains drifted over the electrode surface, the formation of columns was again observed.

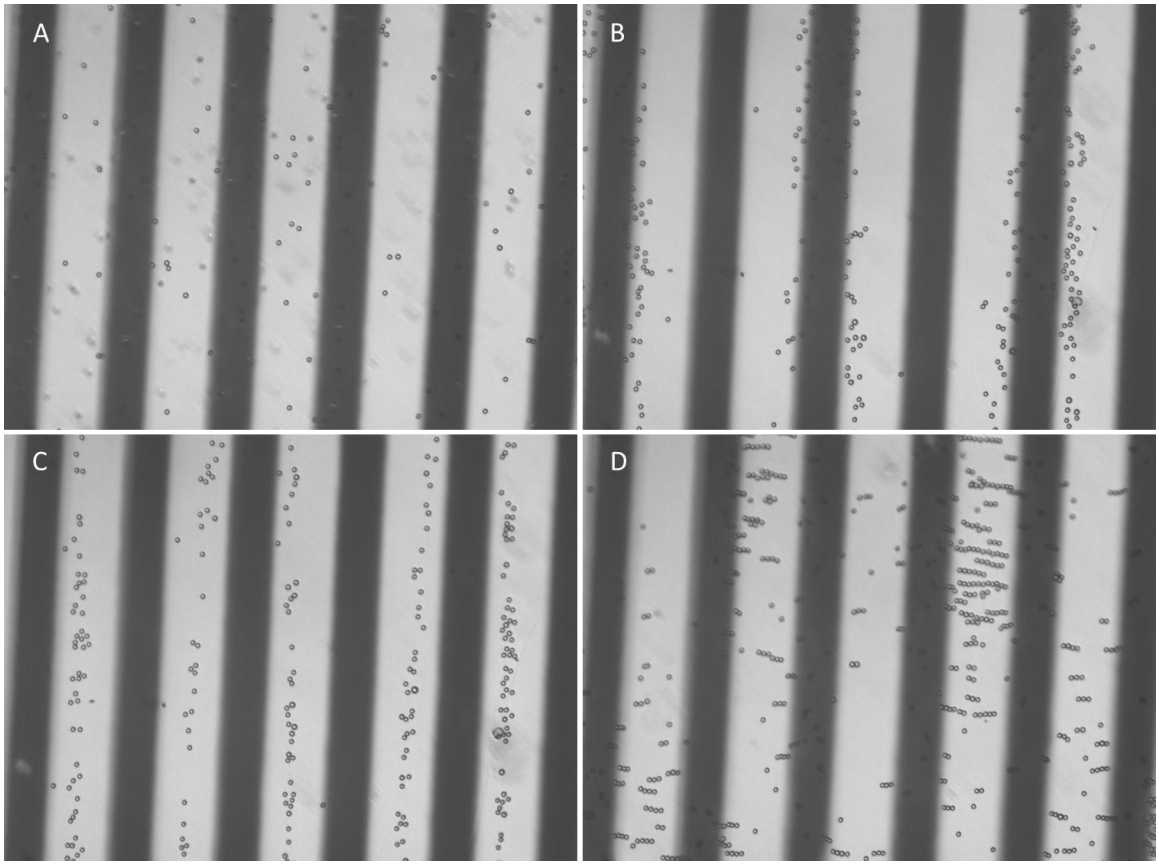

Figure 6.6: 4.5µm beads, 50µm electrode;
no potential (A), 50kHz (B), 160kHz (C), 20MHz (D)

At around 50kHz, the 10µm beads began to aggregate and form pearl chains between every other pair of electrode digits as shown in **Figure 6.7** below. This grouping of pearl chains became increasingly well-defined until there were virtually no beads present anywhere except between these alternating pairs of electrodes at 120kHz. Sufficient beads aggregated such that some groupings of pearl chains became so dense

that individual chains could no longer be distinguished. Around 300kHz the beads were lifted off of the LDPE substrate. This time they largely remained in the alternating spaces between the electrodes. The pearl chains remained discernible until 17MHz. At this point the beads between alternating electrode digits became loose aggregations and some began to drift out of this pattern of alignment. This trend continued until the study was terminated at 20MHz.

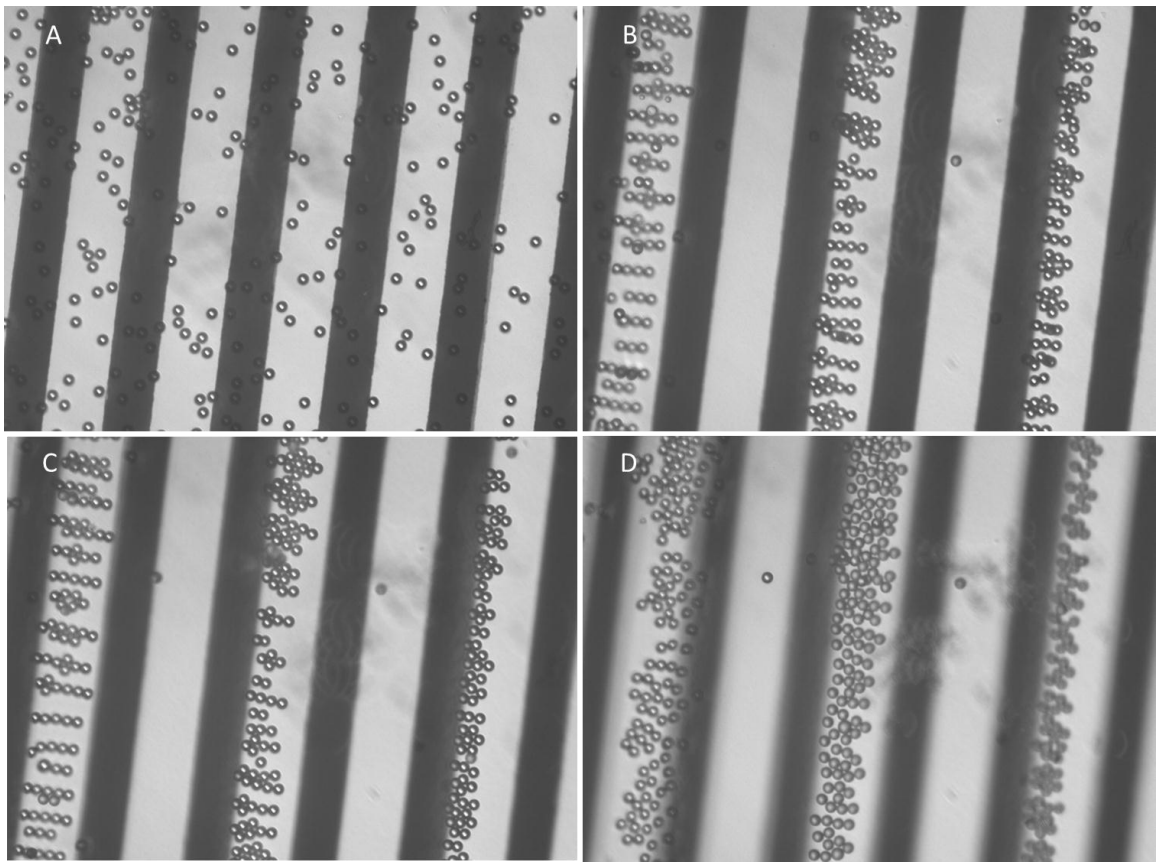

Figure 6.7: 10µm beads, 50µm electrode;
no potential (A), 150kHz (B), 800kHz (C), 17MHz (D)

6.1.8 Results for Frequency Sweep with LDPE Sheet: Low Voltage Large Electrode Geometry

At this lower voltage the hope was that the beads would not be lifted so quickly off of the substrate due to the weaker field. This would likely allow for a larger range of controllable pearl chain formation. This hypothesis was proven to largely be true according to the results described here.

The response of the 2μm beads at 20kHz was barely noticeable, but at 30kHz pearl chains began to form in the center of the spaces between the electrode digits. Pearl chain formation peaked at about 200kHz. From this point the chains became more crooked and began to break down. Some of the beads lifted off of the substrate beginning at 300kHz. From 1MHz onward, there was little sign of pearl chain arrangement, and some of the beads that had been lifted between the electrode digits came to rest in the regions directly above them. The density of beads on the electrodes increased until about 2.5MHz. At this point the beads began to drift away from the regions above the electrodes and distribute themselves randomly through the surface portion of the media. When the study was terminated at 20MHz, there were virtually no beads resting on the substrate, and most were randomly distributed throughout the solution.

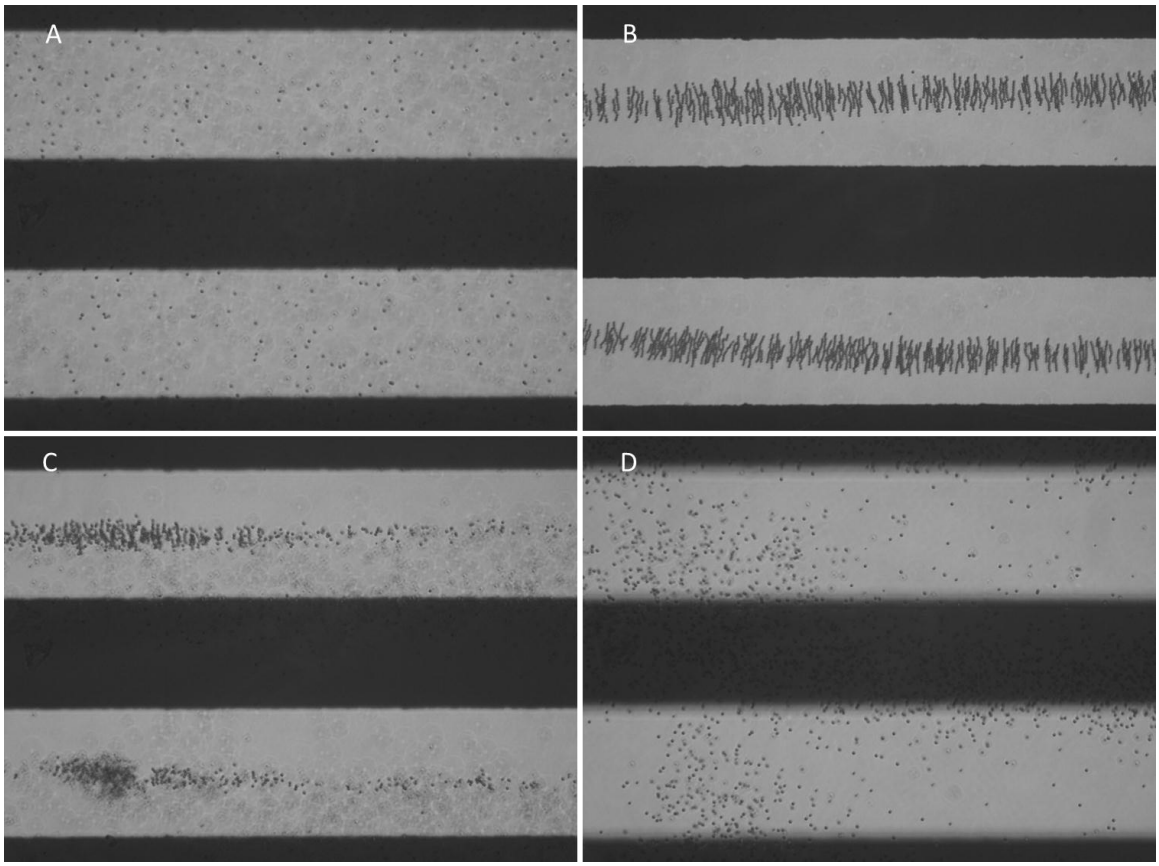

Figure 6.8: 2µm beads, 110µm electrode;
no potential (A), 200kHz (B), 1MHz (C), 20MHz (D)

The 4.5µm diameter beads responded very little until about 60kHz. At this point they began to loosely aggregate between the electrode digits. Discernible pearl chains did not form until about 100kHz. Pearl chain formation continued, and they became very straight and defined at 700kHz. These chains continued to lengthen and remained straight and separate but also began to lift around this point. A small amount of the pearl chains drifted out of the spaces between the electrode digits to the regions above the electrodes beginning at about 1.15MHz. The majority of the pearl chains remained between the electrode digits and remained very well defined until 6MHz. At some frequency between

5MHz and 6MHz the forces holding the pearl chains together was greatly diminished and the individual beads began to drift apart. The pearl chains that had drifted onto the electrodes had formed columns, but these also broke down at this same frequency. The beads remained in loose aggregations between the electrode digits until the study was terminated at 20MHz.

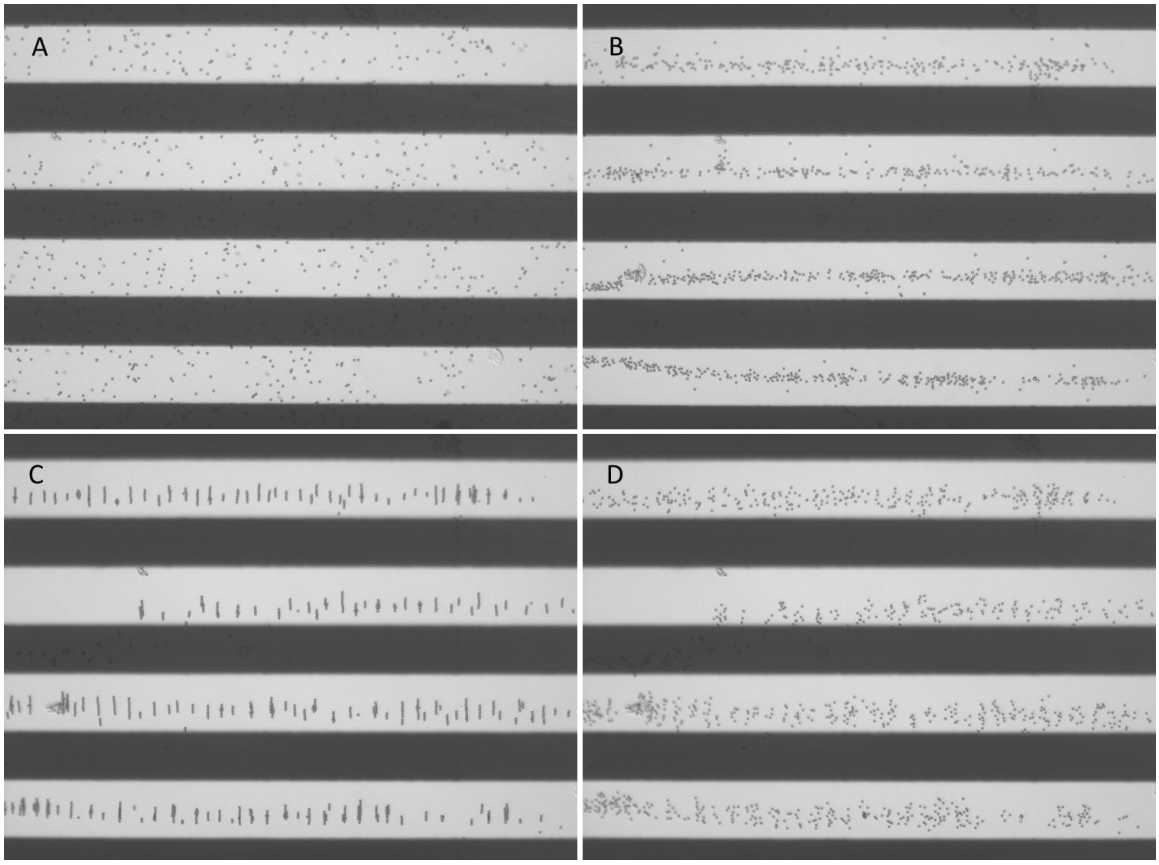

Figure 6.9: 4.5µm beads, 110µm electrode;
no potential (A), 100kHz (B), 5MHz (C), 20MHz (D)

The breakup of the pearl chains was so sudden that it was thought that perhaps the function generator had become disconnected. In order to test this, the frequency was lowered back to 5MHz, the point immediately before the breakup of the pearl chains. This caused the pearl chains to re-form just as they had been earlier in the study.

10μm microspheres exhibited an even larger range of coherent pearl chain formation under low voltage conditions. Pearl chain formation began at 50kHz, but was not complete until about 100kHz. Some of these larger beads always remained on the electrode digits, the only thing that changed as the frequency rose was that they became more evenly spaced. The pearl chains did not break down and were not noticeably lifted even at 20MHz. The only thing that changed was that the beads on the electrode surface were forced closer to the center line of each electrode digit as can be seen in **Figure 6.10**.

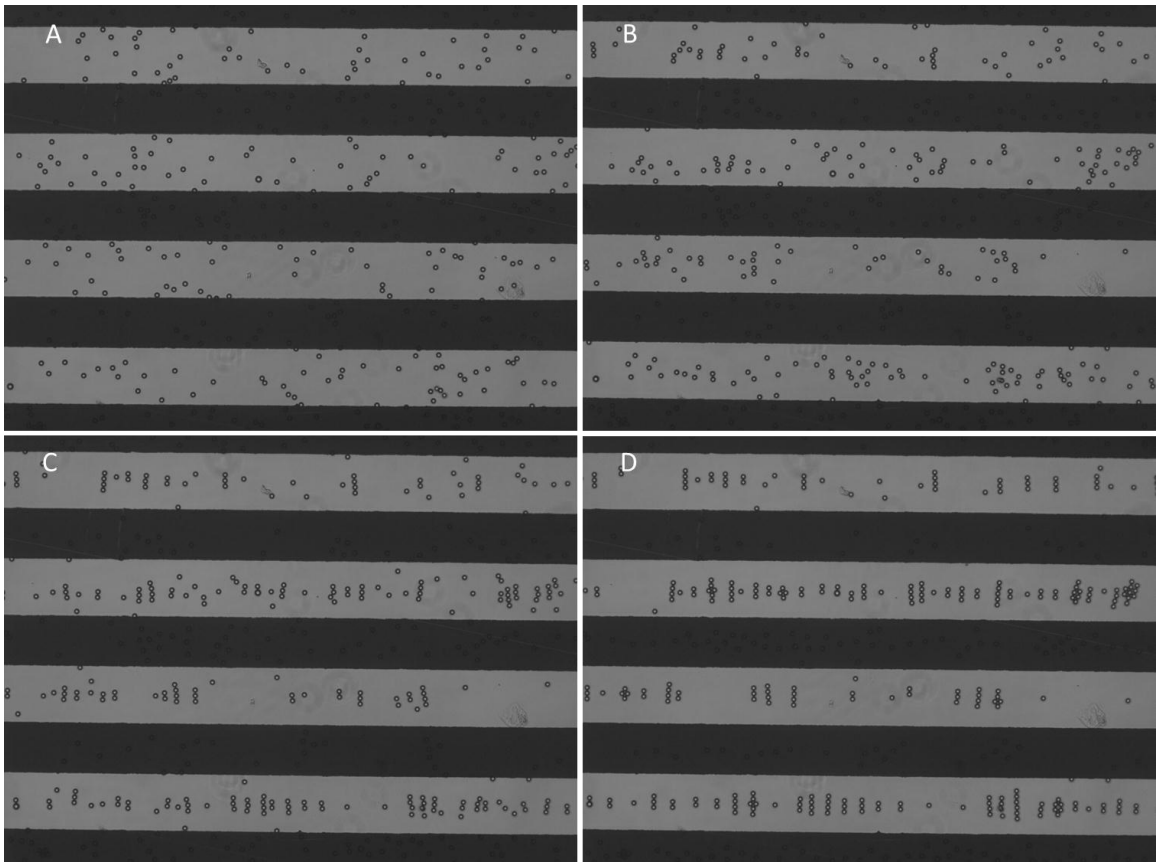

Figure 6.10: 10µm beads, 110µm electrode;
no potential (A), 50kHz (B), 100kHz (C), 1.2MHz (D)

6.1.9 Conclusions:

It is definitely possible to perform insulated negative dielectrophoresis with polystyrene microspheres with voltages lower than 32Vpp using our setup. In fact it is better to use a somewhat lower voltage because the pearl chains form over a larger frequency range. The relatively high voltage of 32Vpp produced too strong a field for negative dielectrophoresis in many cases. This is especially true for smaller beads and smaller spaces between electrode digits. The smaller beads are less massive, and

therefore are more easily displaced. Smaller spaces between electrode digits would mean more force is applied to the particles due to the stronger electric field.

The observed flow patterns were determined to not be a result of phenomena induced by the electrodes such as electro-osmosis or joule heating. They were instead determined to be due to capillary action. When the glass coverslip forming the top of the fluid chamber was not level, the microsphere suspension would flow toward regions where the space between the coverslip and the LDPE sheet was slightly smaller.

CHAPTER SEVEN

DIELECTROPHRESIS FORCE DETERMINATION

7.1 Voltage Sweep with LDPE Sheet

7.1.1 Purpose:

This study is carried out in order to quantify the lifting force related to negative dielectrophoresis. The action of this force was observed in the previous study examining frequency dependent behavior. According to these observations and the governing equations it is hypothesized that if bead size and electrode geometry remain constant, the voltage required to lift the beads off of the electrode surface will decrease with increasing frequency.

Once the voltage at which the lifting takes place for a certain frequency, it can be plugged into **Equation 19** below along with other experimental parameters. The value for the z-component of the dielectrophoretic force at each combination of frequency and voltage can be determined based on the net weight of the lifted microsphere in solution.

7.1.2 Materials for Voltage Sweep with LDPE Sheet:

1. Patterned Electrodes
2. Glass Slide
3. Glass Spacers
4. Glass Coverslip
5. LDPE Sheet
6. Copper Tape

7. Double Sided Tape
8. 10µm Diameter Polystyrene Microspheres (Polysciences, Inc. Polybead®)
9. DI water
10. Wavetek Model 190 20MHz Function Generator
11. Tektronix TDS 1001C-EDU Oscilloscope
12. ZEISS Axiovert® S100 Inverted Microscope
13. JENOPTIC ProgRes® Speed XT Core 3 Camera
14. JENOPTIC ProgRes® CapturePro 2.8 Software

7.1.3 Methods for Voltage Sweep with LDPE Sheet:

The electrode with 50µm spacing and digit width is attached to a glass slide with double sided tape. Two pieces of copper tape are cut measuring 3cm × 0.5cm and are attached to the contact pads of the electrode. The setup is then constructed as shown in **Figure 4.5** using a 1:20 dilution of 15µm diameter polystyrene microspheres.

A voltage sweep is performed at each of the following frequencies: 200, 300, 500, 600, 800, 1000, 1500, 2000, 5000, 10000, 15000, and 20000kHz. This involves beginning at a relatively low AC voltage, usually 5Vpp. This starting voltage is sometimes raised as the frequency is increased. Pictures of the bead behavior are taken at 1-2V intervals until the voltage is well above where significant lifting is first observed. This process is repeated several times and the resulting voltages at each frequency are averaged to obtain the final values for calculating the dielectrophoretic force.

7.1.4 Results for Voltage Sweep with LDPE Sheet:

Three of these voltage sweeps were performed. The results of all three sweeps were relatively similar and can be seen in **Appendix 1**. In the second sweep there appear to be two peaks, seeming to mean that the levitation voltage does not always decrease with increasing frequency. However, when the three sweeps are averaged, this second peak disappears, and is reduced simply to a region with a slope of a smaller negative value than the potions to the right and left of it. This resulting plot can be seen in **Figure 7.1**.

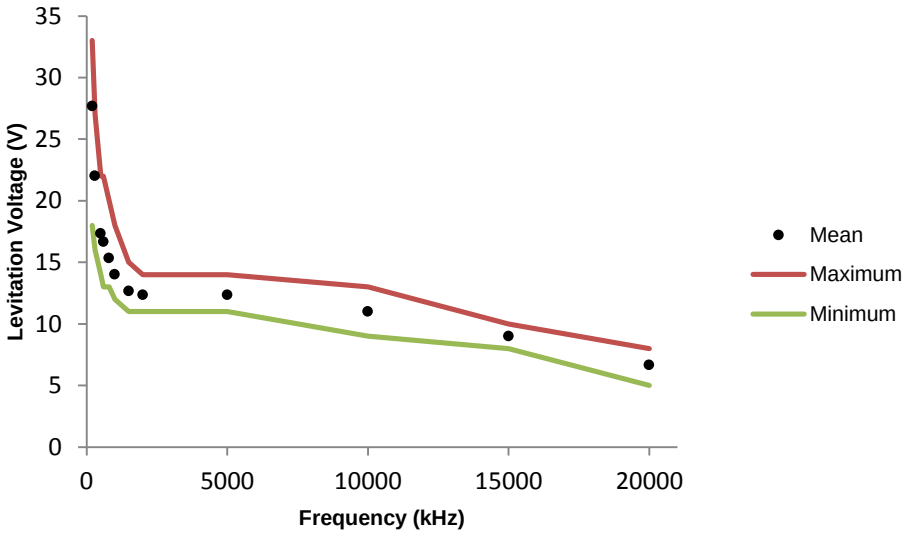

Figure 7.1: Mean levitation voltage vs. frequency, 10µm beads

7.1.5 Conclusions:

It was necessary to repeat this test at least a few times and obtain an average value due to the necessarily qualitative nature of assessing the point of bead levitation and the

possibility of experimental error. This concern is especially valid since this study is intended to produce numerical or quantitative results regarding the magnitude of the dielectrophoretic force in the z-direction.

The results of this study show that it is possible to get a basic idea of the frequency dependence of the dielectrophoretic force in the z-direction. It is also possible to quantify this force by relating it to the weight of the particle in its suspending media. The relative weight of the particle plus the drag force is equal to the lifting force just as it leaves the substrate. At the moment in which the z-component of the dielectrophoretic force is equal to the net weight of the particle in solution, it is not yet in motion, thus lifting cannot be observed. Once lifting is observed, there is some drag force on the bead. The resulting equation is quite simple (**Equation 18** below).

$$|F_{DEPz}| = F_w - F_b + F_d \tag{18}$$

$$|F_{DEPz}| = \frac{4}{3}\pi r_p^3 g\left(\rho_p - \rho_f\right) + \frac{1}{2}\rho v^2 C_D A \tag{19}$$

Equation 18 simply shows that the force due to dielectrophoresis is equal to the difference of the weight of the particle and the buoyant force plus the drag force. **Equation 19** is the combination of these forces using variables that are known for this experiment (apart from the velocity of the bead). The single value produced by **Equation 19** is the value of the dielectrophoretic force required to begin bead levitation. The theoretical equation for the z-component of the dielectrophoretic force is **Equation 20** below.

$$F_{DEPz} = 2\pi r_p^3 \varepsilon_f \left(\frac{\omega^2(\varepsilon_p - \varepsilon_f)(\varepsilon_p + 2\varepsilon_f) + (\sigma_p - \sigma_f)(\sigma_p + 2\sigma_f)}{\omega^2(\varepsilon_p + 2\varepsilon_f)^2 + (\sigma_p + 2\sigma_f)^2} \right) \left| \frac{\partial E}{\partial z} \right|^2 \quad (20)$$

Using the frequency and voltage pairs for the coordinates in **Figure 7.1**, **Equation 20** should produce a relatively constant value. This however is not the case, meaning either that the equation is inadequate in itself, or there are other forces at work in the experimental setup that are unaccounted for.

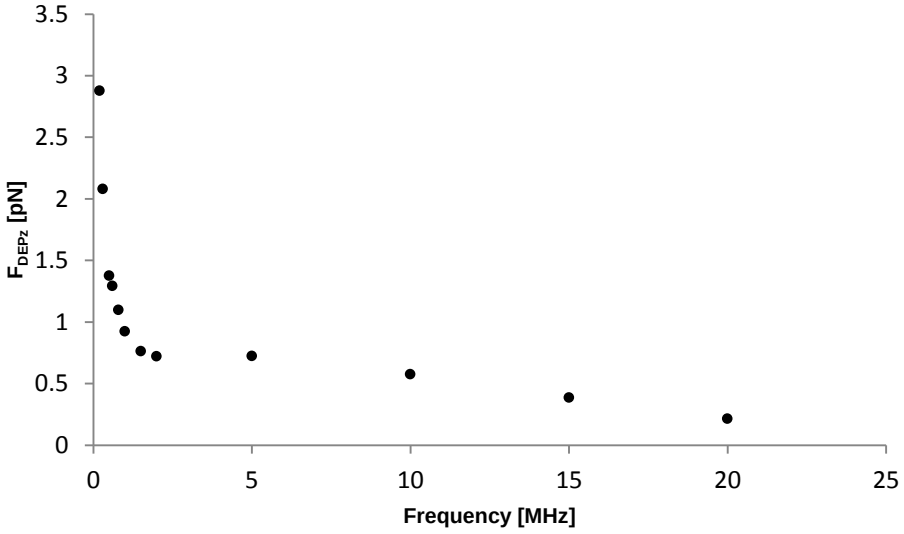

Figure 7.2: Z-direction DEP forces at experimental levitation voltages

It can be seen from **Figure 7.2** that these force values are not the same. Also from **Equation 19**, the weight of the particle is 2.568×10^{-1}pN, which is very close to the smallest force shown in **Figure 7.2** (2.134×10^{-1}pN at 20MHz).

It could be that the exact moment of levitation is not observed. If the beads have lifted only a few microns off of the plastic sheet, then the assumption that they are at their lowest possible point before observable levitation occurs could lead to some of the observed discrepancy. However, the trend exhibited here is too consistent to attribute completely to such experimenter error.

7.2 Variation of Media Conductivity with LDPE Sheet

7.2.1 Purpose:

These studies were performed in order to gauge the effect of media conductivity on particle arrangement. Previous results had shown that neither cells nor beads could be manipulated in very high conductivity cell growth media such as Dulbecco's Modified Eagle Medium. Due to this observation as well as the relative ease of manipulating polystyrene beads in DI water with very low conductivity, it was desired that the effect of conductivity on the effective strength of the dielectrophoretic force should be analyzed at several different conductivities in order to see if a trend developed.

7.2.2 Materials for Variation of Media Conductivity with LDPE Sheet:

1. Patterned Electrodes
2. Glass Slide
3. Glass Spacers
4. Glass Coverslip
5. LDPE Sheet

6. Copper Tape
7. Double Sided Tape
8. 15µm Diameter Polystyrene Microspheres (Polysciences, Inc. Polybead®)
9. DI water
10. NaCl
11. Wavetek Model 190 20MHz Function Generator
12. Tektronix TDS 1001C-EDU Oscilloscope
13. ZEISS Axiovert® S100 Inverted Microscope
14. JENOPTIC ProgRes® Speed XT Core 3 Camera
15. JENOPTIC ProgRes® CapturePro 2.8 Software

7.2.3 Methods for Variation of Media Conductivity with LDPE Sheet:

The straight interdigitated electrode is secured to a glass slide with double sided tape. Two strips of copper tape, 3cm in length and 0.5cm wide, are cut and attached to the contact pads of this electrode. The setup is then constructed as shown in **Figure 4.5** using 1:20 dilutions of 15µm diameter polystyrene beads in DI water and several concentrations of NaCl, These concentrations are of known conductivity.

The test performed here is similar in method to the voltage lift test described above, except this time media conductivity is varied instead of frequency. The function generator is attached and the voltage is set as close as possible to 0Vpp and 20MHz. The voltage is then slowly raised until particle levitation is observed. This voltage is then recorded. This process is repeated for each solution of known conductivity.

7.2.4 Results for Variation of Media Conductivity with LDPE Sheet:

As expected, the voltage necessary to levitate the beads increased with increasing conductivity. This trend can be seen in **Figure 7.3** below.

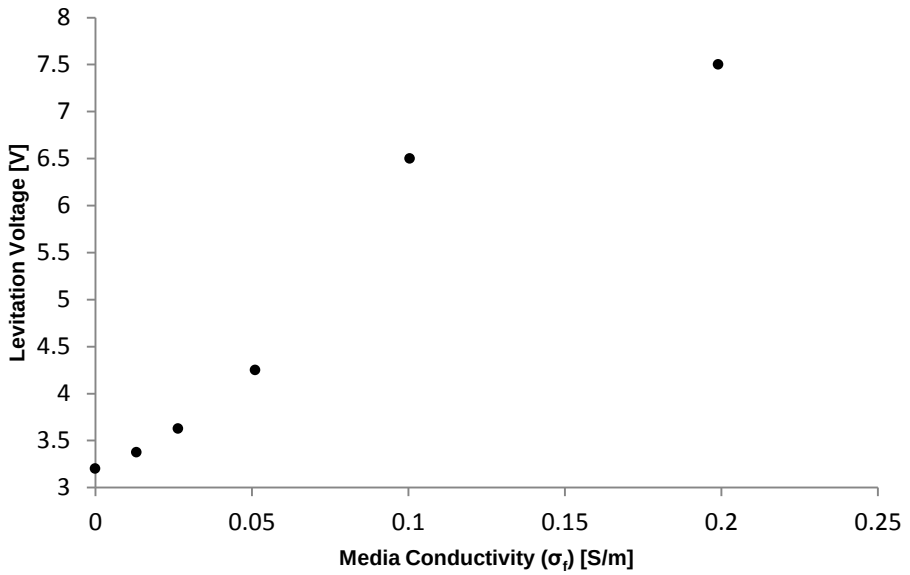

Figure 7.3: Levitation voltages for 15µm beads vs. media conductivity

An equally dramatic trend was noted in the percentage of total beads lifted at the maximum voltage (32Vpp). This decreased sharply with increasing media conductivity. These results are shown in **Figure 7.4**.

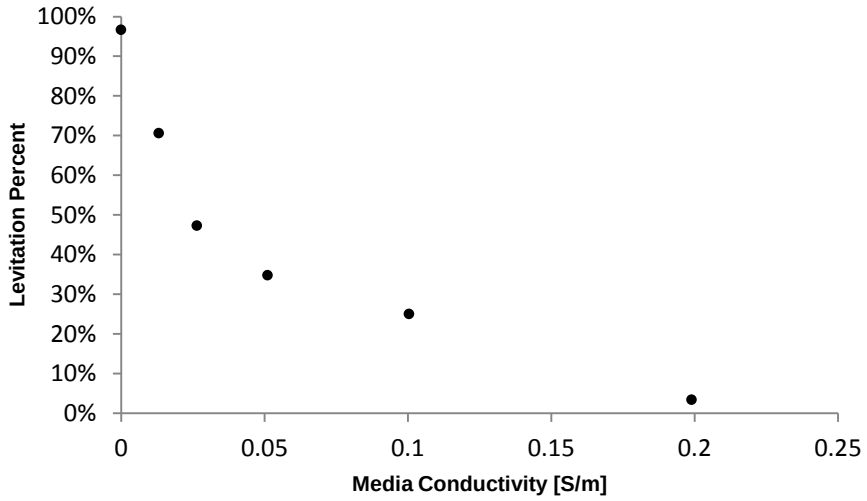

Figure 7.4: Percent of 15µm beads levitated at 32Vpp at various media conductivities

7.2.5 Conclusions:

The reasons for requiring higher voltages to levitate beads in higher conductivity media are likely complex. These could involve the formations of various shielding double-layers or other forces besides dielectrophoresis. A significant observation is that even though the efficiency of dielectrophoresis decreases dramatically as media conductivity rises, there are no signs of electrothermal flow or electro-osmosis, both of which are serious issues for direct media-electrode contact setups.[21]

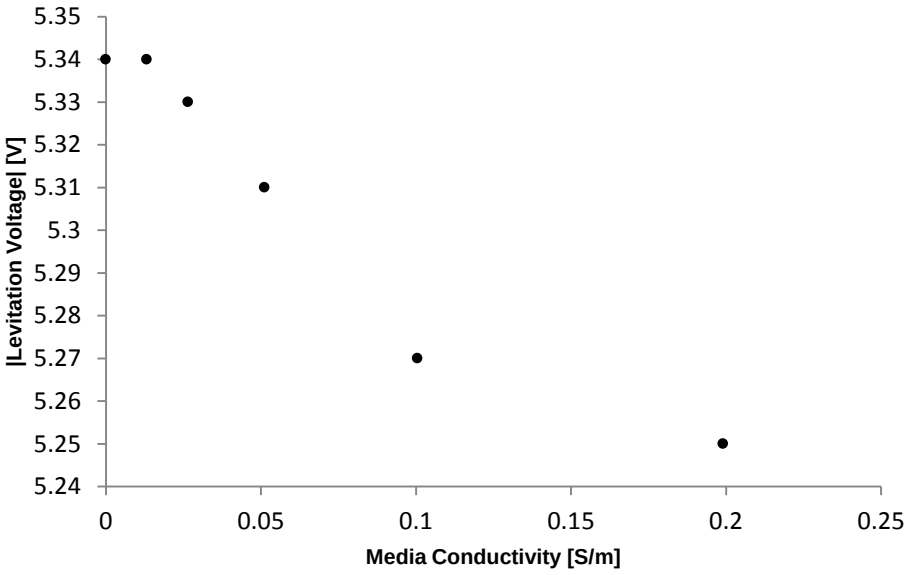

Figure 7.5: Theoretical voltages required to produce 8.668×10^{-1}pN force

Incidentally, the value 8.668×10^{-1}pN is the weight of a 15µm diameter bead in water. Also it is interesting to note that this force value lies almost exactly in the center of the distribution of those determined from the experimental levitation voltages. It can be seen in **Figure 7.5** that the theoretical equation predicts that the required levitation voltage will decrease, with increasing conductivity, though the overall effect is rather small. This is the opposite trend observed in the experimental levitation voltage measurements (**Figure 7.3)**.

Part of the reason for this discrepancy could be due to the fact that it is not likely that all of these other terms in the real part of the Clausius-Mossotti factor remain constant. The fluid permittivity also is likely to increase slightly with increasing conductivity, when the increase in conductivity is due to adding NaCl. This will

somewhat dampen the effect of conductivity on the magnitude of the dielectrophoretic force. However, it is unlikely that this will have an effect significant enough to balance the voltage contribution to the electric field term in **Equation 20** or the effect of increasing media conductivity in the theoretical equation.

As with the experiment discussed in 7.1, experimenter error could also contribute to this discrepancy (if the levitation voltage is not precisely observed), but the reverse in the overall trend is likely not due to only this.

CHAPTER EIGHT

FIELD MAPPING WITH SMALL POLYSTYRENE BEADS

8.1 Mixture of Polystyrene Bead Sizes with SU-8 Coating

8.1.1 Purpose:

The purpose of this study was to investigate the potential for using the SU-8 insulated electrode setup for analyzing the interactions between particles of different sizes. The results of this study make it more valuable for mapping the field around larger particles undergoing dielectrophoresis using smaller particles. It also presents an interesting situation to test the capabilities of COMSOL modeling against experimental reality.

8.1.2 Materials for Mixture of Polystyrene Bead Sizes with SU-8 Coating:

1. Patterned Electrode
2. Glass Slide
3. Glass Spacers
4. Glass Coverslip
5. LDPE Sheet
6. Copper Tape
7. Double Sided Tape
8. 2μm Diameter Polystyrene Microspheres (Polysciences, Inc. Polybead®)
9. 10μm Diameter Polystyrene Microspheres (Polysciences, Inc. Polybead®)
10. DI water

11. Wavetek Model 190 20MHz Function Generator
12. Tektronix TDS 1001C-EDU Oscilloscope
13. ZEISS Axiovert® S100 Inverted Microscope
14. JENOPTIC ProgRes® Speed XT Core 3 Camera
15. JENOPTIC ProgRes® CapturePro 2.8 Software
16. 24V AC to 117V AC transformer

8.1.3 Methods for Mixture of Polystyrene Bead Sizes with SU-8 Coating:

A square interdigitated electrode with alternating 80μm and 120μm spacing and constant digit width of 100μm is coated with a 4μm thick layer of SU-8 photoresist. This electrode is attached to a glass slide using double sided tape. A piece of copper tape measuring 3cm × 0.5cm was attached to each of the electrode's contact pads. The setup is constructed as shown in **Figure 4.6** and as discussed in the accompanying text.

The function generator is attached to the pieces of copper tape and set to 32Vpp. The frequency is swept between 100kHz and 2MHz. For voltages below 300kHz, the transformer was attached for a few tests and AC voltages of up to 230Vpp were applied to the setup. Pictures are taken at several points during this process to document bead behavior.

8.1.4 Results for Mixture of Polystyrene Bead Sizes with SU-8 Coating:

At this voltage and frequency range using the SU-8 coated setup, there was very little if any response elicited from the 10µm diameter polystyrene beads. They remained randomly distributed and were not levitated off of the SU-8 surface.

The same was not true for the 2µm microspheres. These were largely held completely off of the SU-8 surface due to dielectrophoresis. The loose aggregations of these beads were concentrated over the electrode surfaces and the spaces between electrode digits (there were not many along the electrode borders). These aggregations were most dense in the spaces between digits where there was a 90° bend as shown in **Figure 8.1** below.

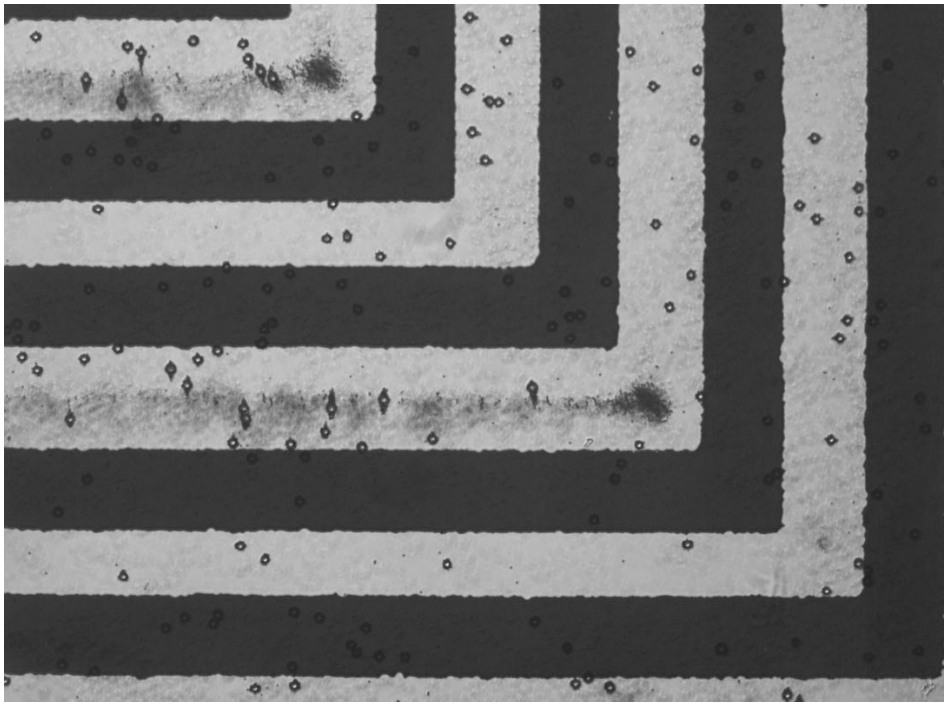

Figure 8.1: Antennae of 2µm beads on 10µm beads at 32Vpp, 2MHz

In addition to this, some of the 2µm diameter beads aggregated around the larger ones. These beads sometimes formed antennas which extended out from the larger microspheres, perpendicular to the electrode digits, in both directions as shown in Figure **8.1**. Other large beads appeared to be randomly spiked with 2µm beads, though the arrangement did somewhat seem to favor the XY-plane. This arrangement can be seen best in **Figure 8.2**.

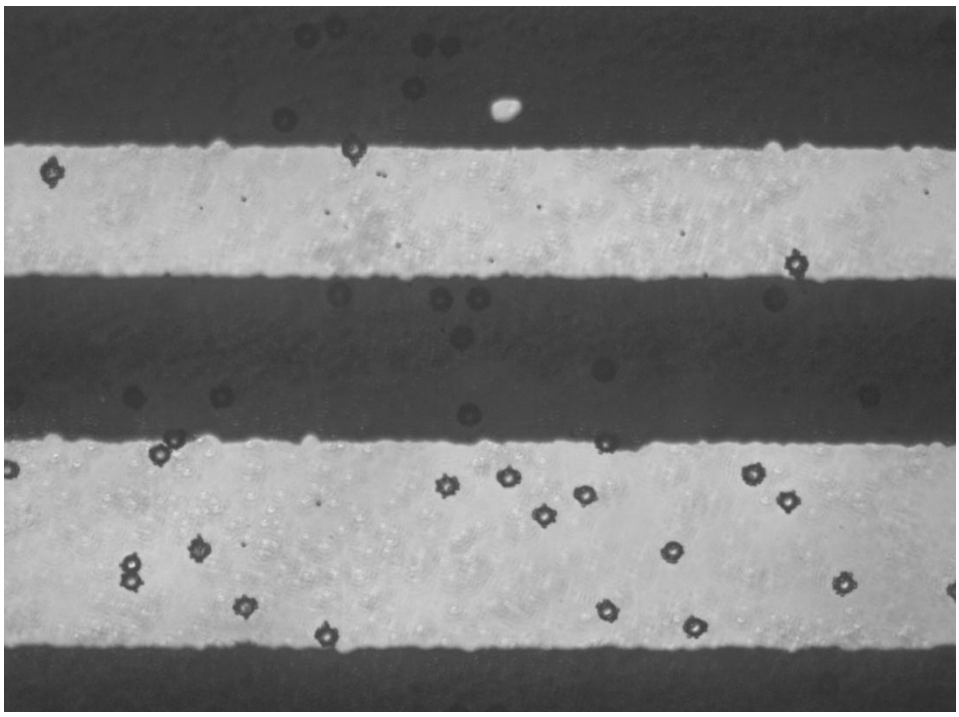

Figure 8.2: Random attachment of 2µm beads to 10µmbeads at 32Vpp, 2MHz

It is also important to note the alternating presence of the 2µm diameter beads between electrode digits. It is only between digits which are slightly farther apart that the small beads aggregate. It is also between these digits that the antennae are able to form.

At lower frequency and much higher voltage ~200Vpp, the 2µm beads behaved quite differently. They group most densely close to the electrode surface and at the electrode edges on either side of the more narrow gaps.

In addition to this difference, the small beads form antennae extending from the larger beads parallel to the electrode digits. These antennae are not as long as those which form at high frequency conditions, but are still visible in **Figure 8.3** below.

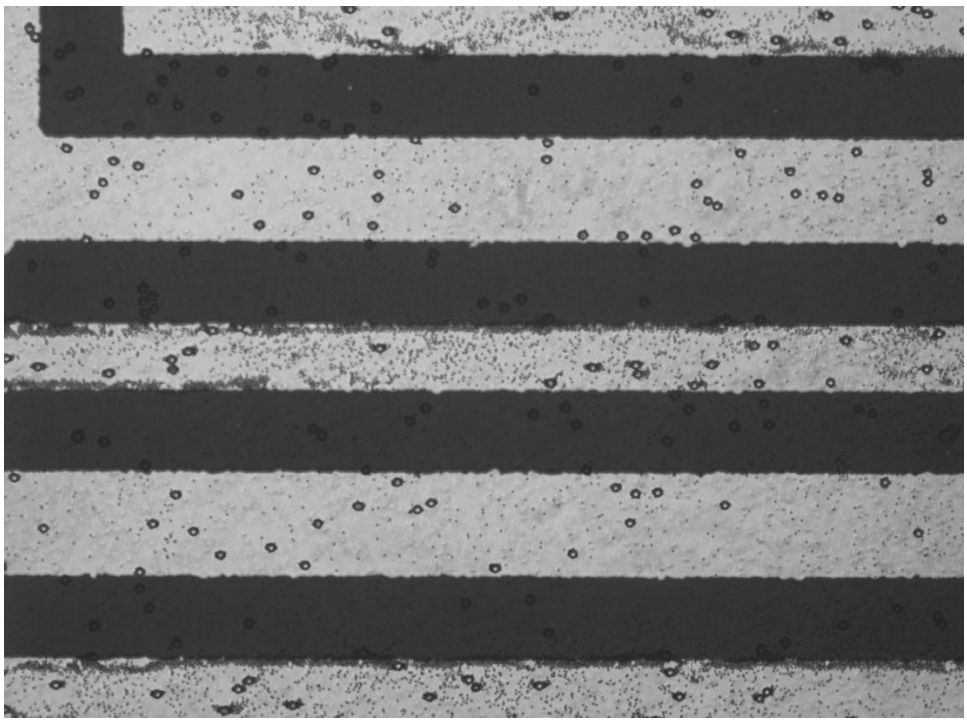

Figure 8.3: Mixture of 10µm and 2µm microspheres at 100kHz and 200Vpp

8.1.5 Conclusions:

It is most likely the case that the larger polystyrene beads are altering the electric field strength in the regions surrounding them such that regions of lower field strength are

created in the areas immediately between themselves and the electrode digits on either side. The smaller beads are able to aggregate in these regions due to negative dielectrophoresis. A similar phenomenon is responsible for the smaller beads' grouping mainly over the electrodes with larger spacing. The field strength is inversely proportional to the square of distance, so regions with larger electrode spacing will have lower field strength and will better foster negative dielectrophoresis.

The opposite trend observed at lower frequency seems to be due to a transition point occurring in the Clausius-Mossotti factors of at least the smaller beads. The smaller beads clearly exhibit positive dielectrophoresis with their aggregation at the electrode edges. Their interactions with the larger beads is being studied further, but according to the results of Mehrle et al. and our current COMSOL simulations, it is likely that for some reason the larger beads have not undergone the same transition.[20] This seems odd due to the assumption that these two sizes of bead have the same composition and should therefore have the same complex permittivities. However, this still seems to be what is happening.

Particles of high permittivity create regions of high electric field strength in the areas perpendicular to themselves and the electrode digits on either side. These particles also create regions of low field strength around their equators parallel to the electrode digits.[20] This basic distribution is illustrated in the COMSOL simulation below in **Figure 8.4**. The red areas are of higher field strength and the blue areas correspond to regions of weaker electric field. Incidentally, this bead has been given the permittivity value of polystyrene (~2.5) and the surrounding area has been prescribed that of water at room

temperature (~80). So this image would be an example of the opposite situation described by Mehrle, a particle with lower permittivity than the surrounding media. The field producing potential difference is from top to bottom in this image.

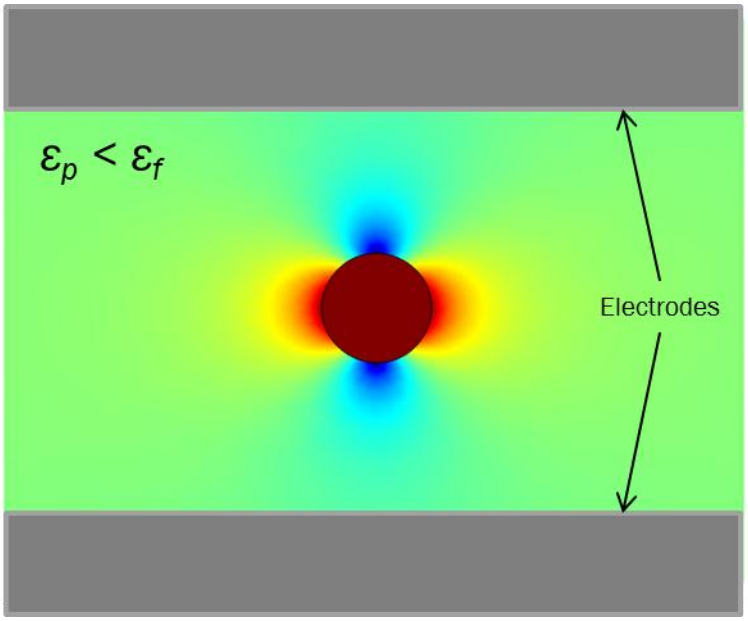

Figure 8.4: COMSOL simulation of low ε_r particle's effect on electric field strength

This would mean that if the 10µm particles are still of lower permittivity than the surrounding media, then a region of higher field strength should be created around their equator parallel to the electrodes on either side. This field distribution corresponds to the 2µm bead arrangement exhibited at lower frequencies.

CHAPTER NINE

DIELECTROPHORESIS OF CELLS

9.1 Positive Dielectrophoresis of Cells with SU-8 Coating

9.1.1 Purpose:

The alignment and manipulation of cells and other biological media is the end goal of this project. Our system has demonstrated the ability to predictably align polystyrene microspheres due to negative dielectrophoresis. The system has been extensively analyzed through experimentation and COMSOL Modeling. It is important to demonstrate its efficacy in dielectrophoretically manipulating cells. The study outlined here is intended only to show that this is possible, and is not an extensive analysis of the underlying physics. This is a preliminary attempt to study the behavior of mammalian cells as a part of our insulated dielectrophoresis system.

9.1.2 Materials for Positive Dielectrophoresis of Cells with SU-8 Coating:

1. Patterned Electrodes
2. Rat Adipose Stem Cells in DMEM
3. Glass Slide
4. Glass Spacers
5. Glass Coverslip
6. LDPE Sheet
7. Copper Tape
8. Double Sided Tape

9. DI water
10. D-glucose
11. Sucrose
12. Wavetek Model 190 20MHz Function Generator
13. Tektronix TDS 1001C-EDU Oscilloscope
14. ZEISS Axiovert® S100 Inverted Microscope
15. JENOPTIC ProgRes® Speed XT Core 3 Camera
16. JENOPTIC ProgRes® CapturePro 2.8 Software
17. 24V AC to 117V AC transformer

9.1.3 Methods for Positive Dielectrophoresis of Cells with SU-8 Coating:

A square interdigitated electrode with alternating 80µm and 120µm spacing and constant digit width of 100µm is coated with a 4µm thick layer of SU-8 photoresist. This electrode is then attached to a glass slide with double sided tape. Two rectangles of copper tape are cut measuring 3cm × 0.5cm and attached to the contact pads of this electrode. The setup is constructed as shown in **Figure 4.6**.

A solution of 8.5% sucrose and 0.3% D-glucose in DI water is prepared. This will be used as the low conductivity media for the RASCs.

Rat adipose stem cells (RASCs) are obtained from storage in liquid nitrogen and slowly brought to room temperature. The 1mL container of cells is to be agitated and its contents are then pipetted into a 15mL tube for centrifugation. The cells are spun down at 1000rpm for five minutes. The supernatant is then removed and discarded. 1mL of the

sucrose/dextrose solution is then pipetted over the cell pellet. The cells are not to be fully re-suspended. This centrifugation and washing procedure is repeated five times. After this is complete the cells should again be agitated to ensure even distribution in the low-conductivity media. A 20µL aliquot of cell suspension is placed on the SU-8 surface as shown in **Figure 4.6**.

The completed setup is then connected to the function generator through the transformer such that the voltage applied to the setup is greater than the voltage supplied by the function generator. The voltage on the function generator is set to the maximum value (32Vpp) and the frequency is swept from 0-5MHz. Images are obtained of the cell response at various voltage and frequency combinations.

It is important to note that there is little danger of damaging the SU-8 coated setup because it passes no current. This is why the transformer can be used to boost the voltage, there is no power supplied through it to the system. Thus as long as the frequency remains relatively low (<100kHz) the transformer will multiply the voltage as indicated (24Vpp raised to 117Vpp). However, this transformer is intended for use at 60Hz, so at much higher frequencies (>100kHz), the core breaks down and its behavior is nonlinear. For example, it produces less than 10Vpp at 20MHz even when the input signal is 32Vpp.

9.1.4 Results for Positive Dielectrophoresis of Cells with SU-8 Coating:

Under the applied conditions, the cells exhibited two major types of behavior. The first of these was at high frequency and is depicted occurring at 5MHz in **Figure 9.1** below.

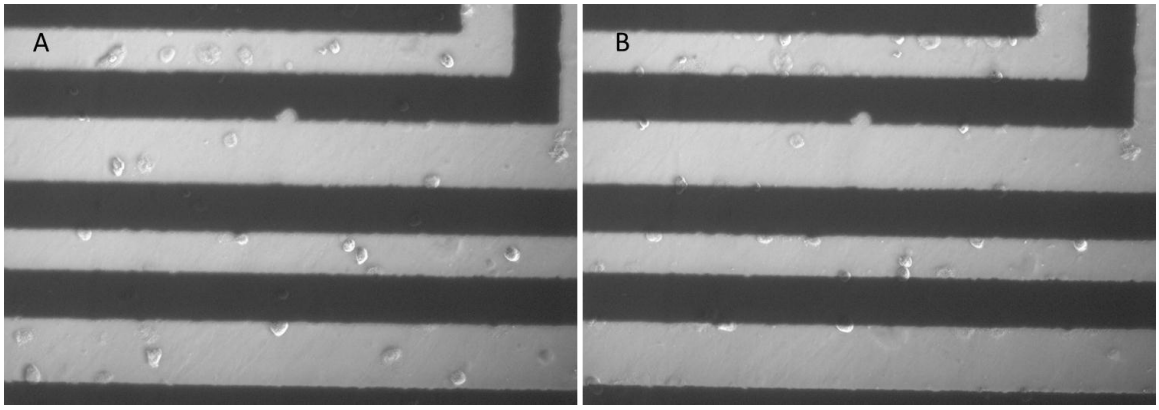

Figure 9.1: RASCs before (A) and after (B) 52Vpp, 4.5MHz is applied

The second type of behavior is more difficult to see in a static image. At low frequency (100-300kHz) several of the cells would rotate. The axes of their respective rotations were sometimes inside the cell and sometimes lied at a point outside the cell making it appear to be orbiting empty space. There was little alignment at these low frequencies, but rotating cells were always observed between electrode digits.

9.1.5 Conclusions:

At high frequency, the cells exhibit positive dielectrophoresis. This behavior is expected and matches the findings of many others.[9, 14, 16, 20, 22] The electric field is strongest at the borders of the interdigitated electrode, and this is primarily where the cells aggregate.

The low frequency behavior was unexpected, but is explainable. COMSOL simulations have shown that this behavior is simply due to asymmetry in the shape of the cell. If the cell is sufficiently asymmetrical and is in the proper position relative to the electrode, the dielectrophoretic forces will act on it in such a way as to induce this rotation. An off-center nucleus further contributes to the overall asymmetry of the cell and also has a significant effect on the cell's rotation according to COMSOL simulations.

CHAPTER TEN

OTHER NOTEWORTHY OBSERVATIONS

10.1 Vertical Pearl Chain Formation and Motion

The first of these observations has been mentioned above in the experimental section, but will now be reiterated. Under normal negative dielectrophoretic conditions polystyrene beads are frequently described as forming pearl chains lying flat on the electrode surface. Cells under the influence of positive dielectrophoresis have also been observed to form something similar to pearl chains extending from electrode edges. Our setup produces a different variety of "pearl chain" due to the action of the same dielectrophoretic forces. These form as vertical columns on the surface of interdigitated electrodes. These are also areas of low field and COMSOL models have demonstrated that this is an energetically favorable arrangement. When the beads are oriented as shown on the electrode digits, in **Figure 10.1**, there is a significant attractive force between them in the vertical direction.

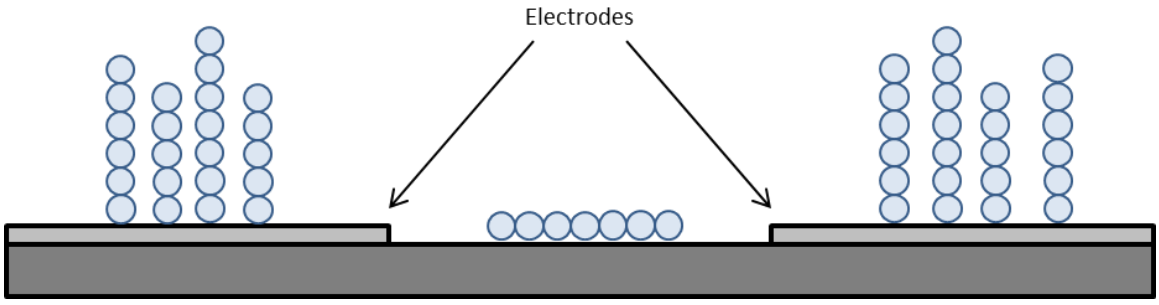

Figure 10.1: Cross section schematic of bead alignment

Figure #: Image of bead columns on electrode digits

When a slow, steady flow is introduced perpendicular to the long axis of the electrode digits, this normally static system becomes quite dynamic. The current washes the pearl chains of both types across the electrode digits as shown in **Figure 4.30**. As chains move across the alternating regions of electrode surfaces and the spaces between, they do not lose their pearl chain arrangement, but instead only change orientation.

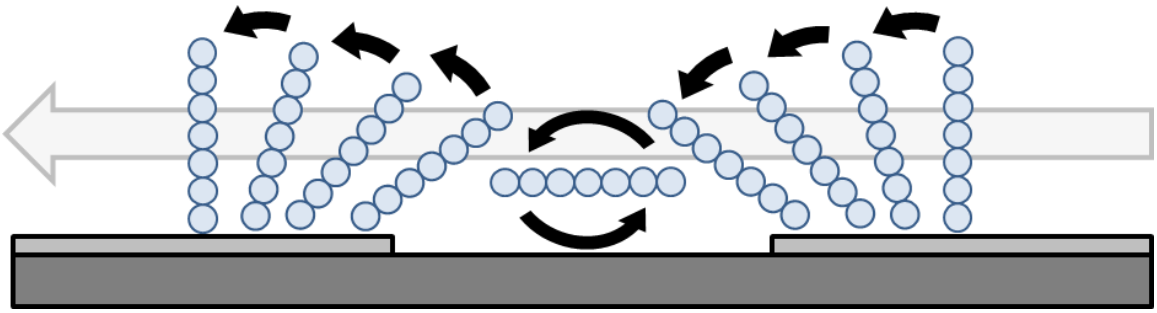

Figure 10.2: Schematic of pearl chain motion in the presence of flow

In **Figure 10.2** the gray arrow indicates the direction of flow while the black arrows indicate the relative motion of the pearl chain as is somersaults across the electrode. At present the observation of such behavior is little more than a curiosity, but there is a possibility that it may be put to use for some purpose in the future.

CHAPTER ELEVEN

META-CONCLUSIONS

When the combined results of all these studies are considered, it can be concluded that the goal of producing a setup for low voltage (or low power) insulated dielectrophoresis has been achieved. This line of experimentation has also provided the fodder for many COMSOL simulations of dielectrophoretic behavior. These models have not been explicitly included due to the fact that I did not construct them. They have simply been mentioned where they are especially helpful in determining the physics underlying various experimental observations.

The major contribution of this line of inquiry to the field as a whole is the quantification of the negative dielectrophoretic force in the z-direction. I have not found any mention of a similar study in my literature search. The nearest extant approximations are studies examining the magnitude of the positive dielectrophoretic force. These studies levitate microparticles toward an electrode suspended above and determine the minimum voltage required for this attraction.[7,8,9,13, 24] This study the analogous action of negative dielectrophoresis may be entirely novel, and it has certainly never been performed with an insulated dielectrophoresis setup.

The observation of a transition point between positive and negative dielectrophoresis using polystyrene beads is not new[25], and is a reflection of the action of the Clausius-Mossotti factor in the equation for dielectrophoretic force. It is, however, interesting that particles assumed to be of the same material composition and only differing in size should exhibit different transition points.

CHAPTER TWELVE

ISSUES FOR FUTURE CONSIDERATION

Many of these experimental results will be combined with the analogous COMSOL models in order to produce more robust elucidation of the dielectrophoretic principles. Agreements between the models and many specific experimental situations will hopefully provide a means for accurately predicting the outcomes of future experiments. This, if taken a step further, could allow for a considerable refinement of the electrode design procedure. The parameters describing the carrying out of a desired operation could be combined with modeling to design electrodes sure to produce the desired results.

In addition to this effort, this setup could be analyzed further in the hope of patterning cells into engineered tissues. Only preliminary cellular studies have been performed with cells, and the system must be more thoroughly analyzed if this goal is to be pursued. In theory both of the insulated electrode setups have their advantages for use in manipulating cells. Cells can be arranged on the thin LDPE membrane removed for use and analysis elsewhere, protecting the electrode and leaving it available for repeated cell alignments. The SU-8 coated electrode is very durable and easy to clean without damaging the electrode. If this design is developed further the life of electrodes used for dielectrophoresis could be greatly extended.

While these setups have been extensively studied, there is a great deal more work to be done. We would like to test particles of different materials, functionalized particles, and hopefully particles of shapes other than spheres. One important issue for further

consideration is the disagreement of the experimentally determined levitation voltages with the theoretical calculation of the dielectrophoretic force in the z-direction. The most likely explanation for this discrepancy is that other forces are at work. It would be very beneficial to include all of the forces discussed in **Chapter 3** in a COMSOL model in order to test whether this is indeed the case. It also may be beneficial to determine the exact height of the beads off of the electrode surface. The assumption that they are touching the insulating layer could contribute significantly to this discrepancy.

It may also be the case that a modified levitation voltage study could be performed using the confocal microscope to determine the height of a bead suspended above the electrode. As long as the height of the bead off of the insulating surface is maintained at a constant value, the weight of the bead could be set equal to the DEP force in the z-direction. Such a study would involve less assumption and may lead to better agreement between theoretical and experimental levitation voltages. Though the study of dielectrophoresis has been continuing in earnest for the past 60 years, there is still a great deal more to be learned.

APPENDICES

Appendix I: Levitation Voltage Plots

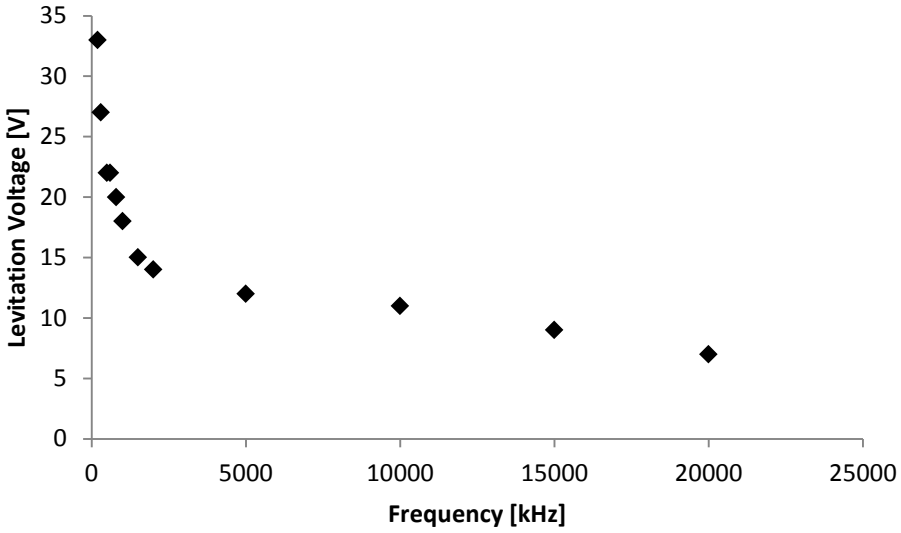

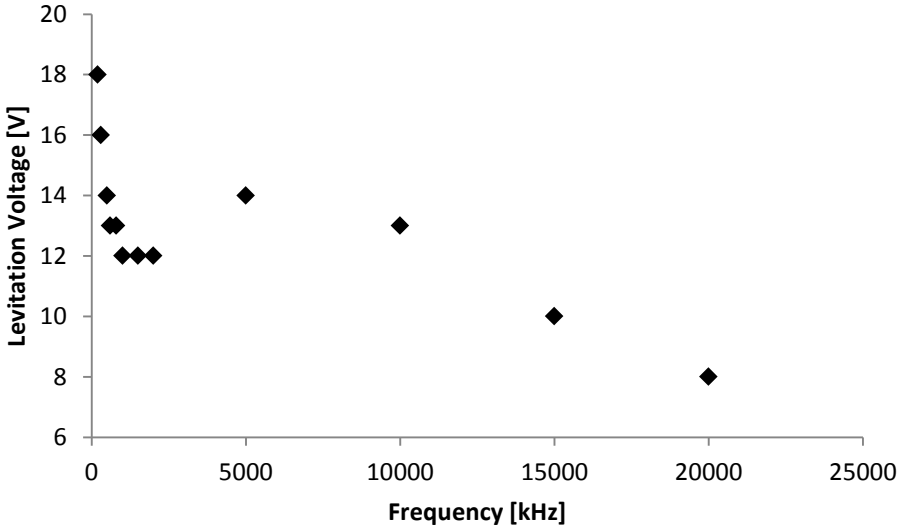

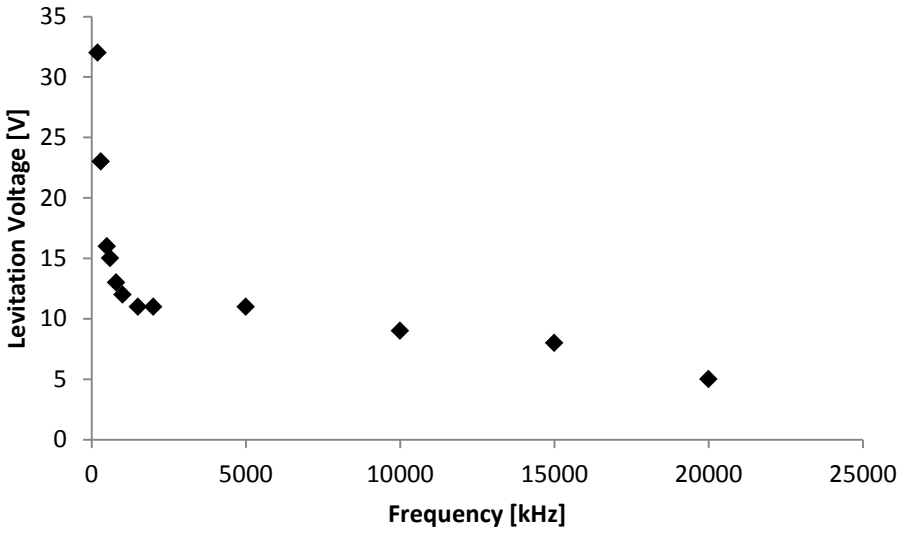
35
30
25
20
15
10
5
0
Levitation Voltage [V]
0
5000
10000
15000
20000
25000
Frequency [kHz]

Appendix II: AFM Surface Characterization of SU-8 Coated Electrodes

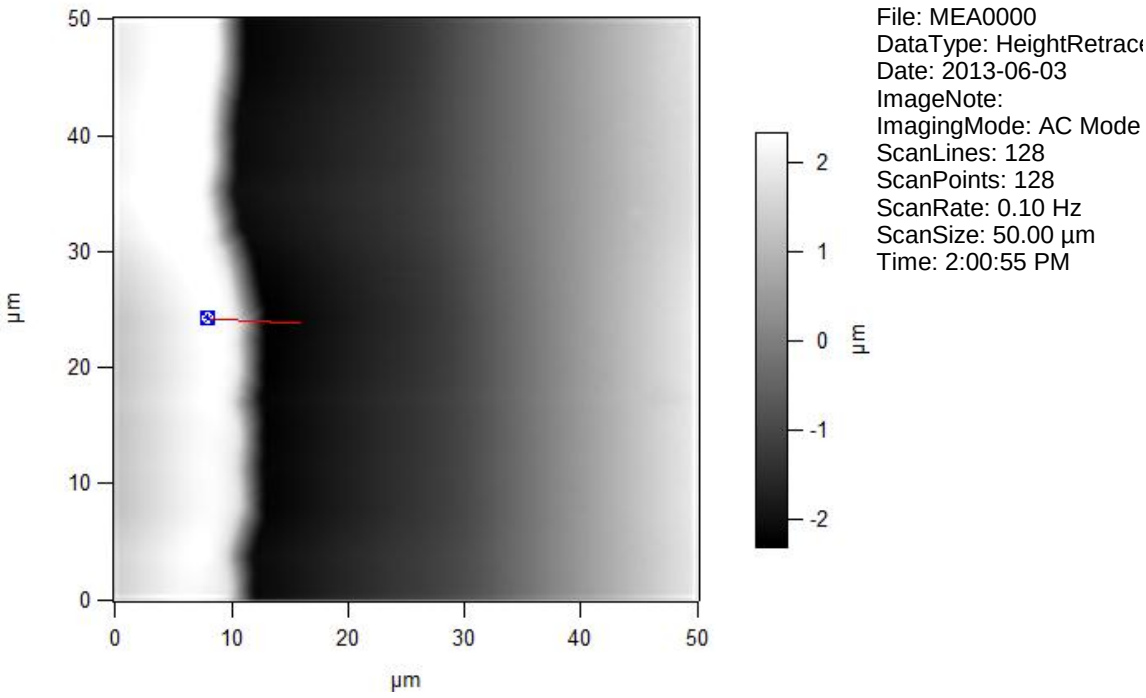

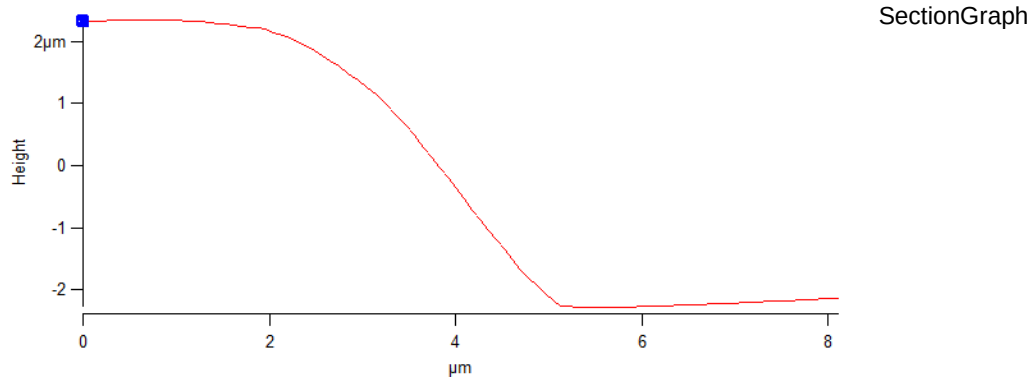

This graph generated from AFM data indicates that the SU-8 coating is about 4µm thick. The white region is the photoresist coating and the dark region is the uncoated portion near one of the electrode's contact pads.

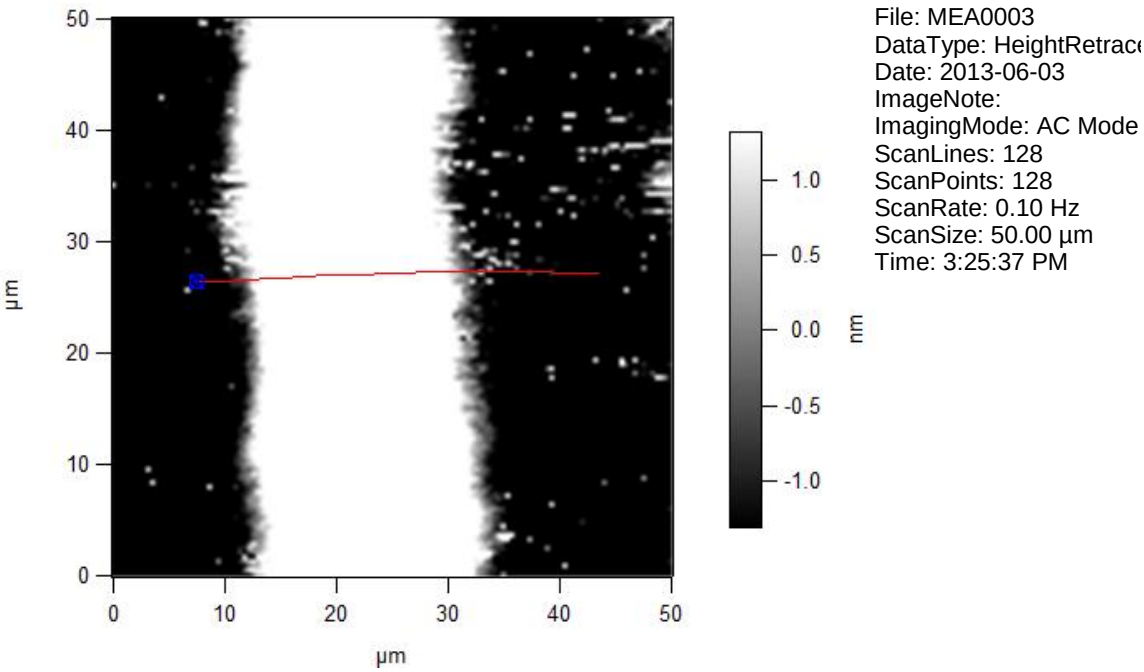

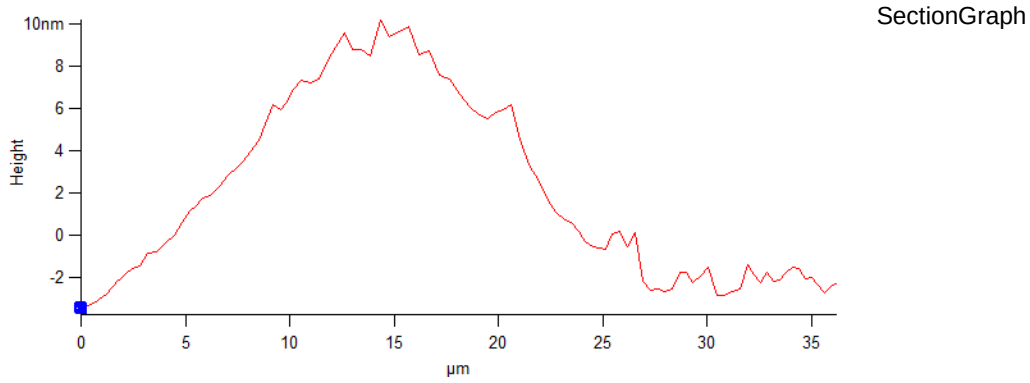

This graph, also from AFM data, shows that the surface of the coating only changes 10nm in height from the trough between the electrode digits to the crest at the center of each digit. This is a very small difference in height considering that the gold and titanium electrode is ~120µm thick under the coating.

Appendix III: Ellipsometric Determination of SU-8 Thickness on Electrode

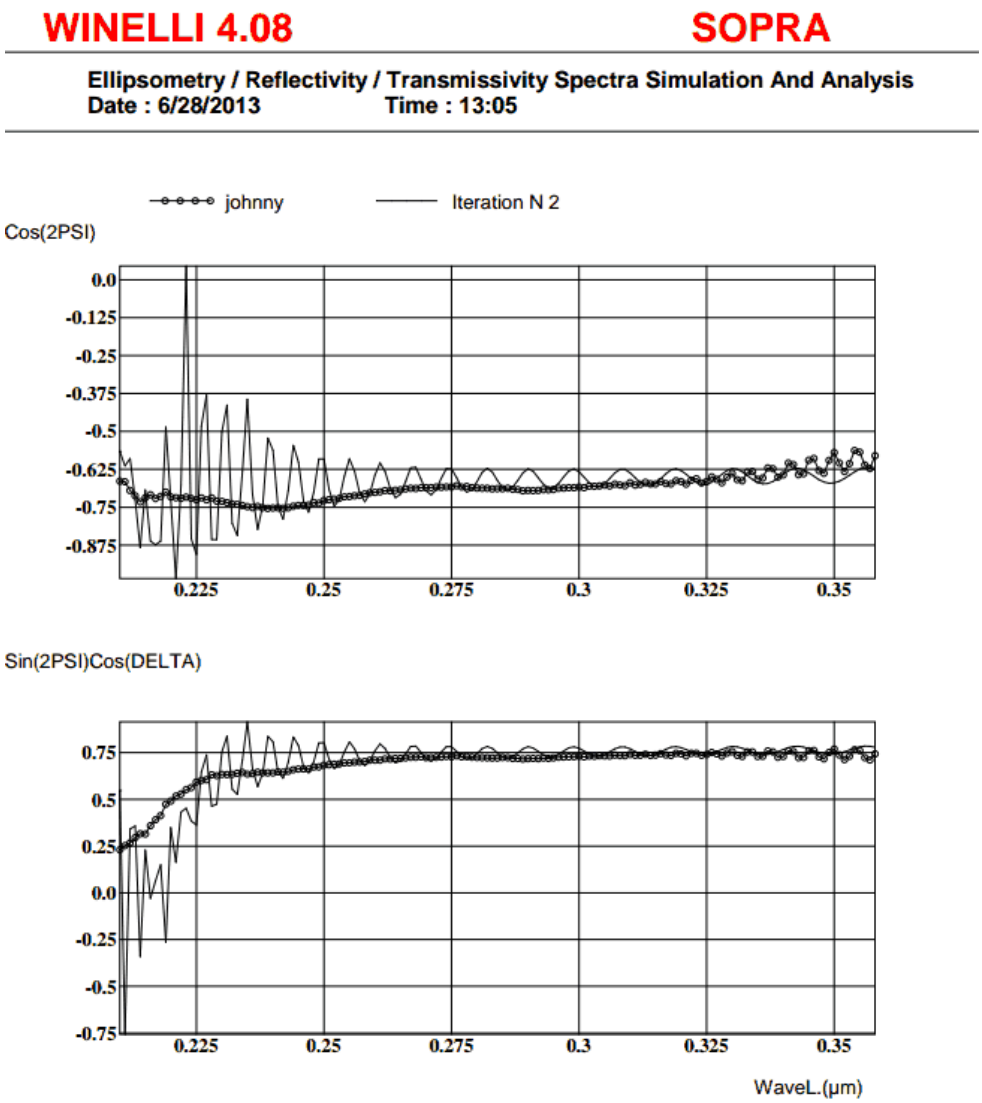

These regression results from ellipsometry data are obtained using the Levenberg-Marquardt algorithm for smoothing the data to fit an accepted model. They indicate that the thickness of the coating is on average 3417.315 ± 3.905nm. This is a much more accurate method of determining the thickness of a thin film than the AFM studies.

REFERENCES

1. Park, K., Suk, H. J., Akin, D., and Bashir, R. (2009). Dielectrophoresis-based cell manipulation using electrodes on a reusable printed circuit board. *Lab on a Chip*. *9*(15), 2224-2229.
2. Fomchenkov, V. M. and Gavrilyuk, B. K. (1978). The study of dielectrophoresis of cells using the optical technique of measuring. *Journal of Biological Physics*. *6*(1-2), 29-68.
3. Fuhr, G., Arnold, W. M., Hagedorn, R., Müller, T., Benecke, W., Wagner, B., and Zimmermann, U. (1992). Levitation, holding, and rotation of cells within traps made by high-frequency fields. *Biochimica et Biophysica Acta (BBA)-Biomembranes*, *1108*(2), 215-223.
4. Maxwell, J. C. (1891). *A Treatise on Electricity and Magnetism*, Vol. 1, 3rd ed., Clarendon Press, Oxford.
5. Pohl, H. A. (1951). The motion and precipitation of suspensoids in divergent electric fields. *Journal of Applied Physics*, *22*(7), 869-871.
6. Pethig, R. (1996). Dielectrophoresis: Using inhomogeneous ac electrical fields to separate and manipulate cells. *Critical Reviews in Biotechnology*, *16*(4), 331-348.
7. Ting, I. P., Jolley, K., Beasley, C. A., and Pohl, H. A. (1971). Dielectrophoresis of chloroplasts. *Biochemica et Biophysica Acta*, *234*, 324-329.
8. Park, S. and Beskok, A. (2008). Alternating current electrokinetic motion of colloidal particles on interdigitated microelectrodes. *Analytical Chemistry*. *80*, 2832-2841.

9. Kaler, K. V. I. S. and Jones, T. B. (1990). Dielectrophoretic spectra of single cells determined by feedback controlled levitation. *Journal of Biophysics*. *57*, 173-182.
10. Kaler, K. V. I. S., Xie, J-P., Jones, T. B., and Paul, R. (1992). Duel-frequency dielectrophoretic levitation of canola protoplasts. *Journal of Biophysics*. *63*, 58-69.
11. Kaler, K. V. I. S., Jones, T. B., and Paul, R. (1995). Low-frequency micromotions of DEP-levitated plant protoplasts. *Journal of Colloid Interface Science*. *175*, 108-117.
12. Washizu, M. and Kurosawa, O. (1990). Electrostatic manipulation of DNA in microfabricated structures. *IEEE Transactions on Industry Applications*. *26*, 1165-1172.
13. Washizu, M., Suzuki, S., Kurosawa, O., Nishizaka, T., and Shinohara, T. (1994). Molecular dielectrophoresis of biopolymers. *IEEE Transactions on Industry Applications*. *30*, 835-843.
14. Fuhr, G., Schnelle, T., Hagedorn, R., and Shirley, S. G. (1995). Dielectrophoretic field cages: technique for cell, virus and macromolecule handling. *Cell. Eng. inc. Molecular Eng*. *1*, 47-57.
15. Jones, T. B. and Washizu, M. (1992). Equilibria and dynamics of DEP-levitated particles: Multipolar theory.
16. Becker, F. F., Wang, X-B., Huang, Y., Pethig, R., Vykoukal, J., and Gascoyne, P. R. C. (1994). The removal of human leukemia cells from blood using

interdigitated microelectrodes. *Journal of Physics D: Applied Physics*. *27*, 2659-2662.

17. Becker, F. F., Wang, X-B., Huang, Y., Pethig, R., Vykoukal, J., and Gascoyne, P. R. C. (1995). Separation of human breast cancer cells from blood by differential dielectric affinity. *Proceedings of the National Academy of Sciences U.S.A. 92*, 860-864.
18. Markx, G. H., Talary, M., and Pethig, R. (1994). Separation of viable and nonviable yeast using dielectrophoresis. *Journal of Biotechnology*. *32*, 29-37.
19. Stephens, M., Talary, M. S., Pehtig, R., Burnett, A. K., and Mills, K. I. (1996). The dielectrophoresis enrichment of CD34+ cells from peripheral stem cell harvests. *Bone Marrow Transplant*. *18*, 777-782.
20. Mehrle, W., Hampp, R., Zimmermann, U., and Schwan, H. P. (1988). Mapping of the field distribution around dielectrophoretically aligned cells by means of small particles as field probes. *Biochimica et Biophysica Acta (BBA)-Biomembranes*. *939*(3), 561-568.
21. Park, S., Koklu, M., and Beskok, A. (2009). Particle trapping in high conductivity media with electrothermally enhanced negative dielectrophoresis. *Analytical Chemistry*. *81*(6), 2303-2310.
22. Ho, C. T., Lin, R. Z., Chang, W. Y., Chang, H. Y., and Liu, C. H. (2006). Rapid heterogeneous liver-cell on-chip patterning via the enhanced field-induced dielectrophoresis trap. *Lab on a Chip*. *6*(6), 724-734.

23. Jones, T. B. (2003). Basic theory of dielectrophoresis and electrorotation. *IEEE Engineering in Medicine and Biology Magazine*. *November/December*, 33-42.
24. Wu, X., Warsynski, P., and van de Ven, T. G. M. (1996). Electrokinetic lift: Observations and comparisons. *Journal of Colloid Interface Science*. *180*, 61-69.
25. Green, N. G. and Morgan, H. (1999). Dielectrophoresis of submicrometer latex spheres. 1. Experimental results. *The Journal of Physical Chemistry B*. *103*(1), 41-50.